A Theoretical Study of the Reaction Mechanism and Product Branching Ratios of C$_2$H + C$_2$H$_4$ and Related Reactions on the C$_4$H$_5$ Potential Energy Surface[†]

Sergey P. Krishtal and Alexander M. Mebel*

Department of Chemistry and Biochemistry, Florida International University, Miami, Florida 33199

Ralf I. Kaiser

Department of Chemistry, University of Hawai'i at Mānoa, Honolulu, Hawai'i 96822

Received: April 30, 2009; Revised Manuscript Received: June 25, 2009

Ab initio and density functional RCCSD(T)/cc-pVQZ//B3LYP/6-311G** calculations of various stationary points on the C$_4$H$_5$ global potential energy surface have been performed to resolve the C$_2$H + C$_2$H$_4$ and C$_2$H$_3$ + C$_2$H$_2$ reaction mechanisms under single-collision conditions. The results show vinylacetylene + H as the nearly exclusive products for both reactions, with exothermicities of 26.5 and 4.3 kcal/mol, respectively. For C$_2$H + C$_2$H$_4$, the most important mechanisms include a barrierless formation of the CH$_2$CH$_2$CCH adduct c6 (56.9 kcal/mol below the reactants) in the entrance channel followed either by H loss from the vicinal CH$_2$ group via a barrier of 35.7 kcal/mol or by 1,2-H migration to form CH$_3$CHCCH c3 (69.8 kcal/mol lower in energy than C$_2$H + C$_2$H$_4$) via a 33.8 kcal/mol barrier and H elimination from the terminal CH$_3$ group occurring with a barrier of 49.4 kcal/mol. RRKM calculations of energy-dependent rate constants for individual reaction steps and branching ratios for various channels indicate that 77−78% of vinylacetylene is formed from the initial adduct, whereas 22−21% is produced via the two-step mechanism involving the 1,2-H shift c6-c3, with alternative channels contributing less than 1%. The theoretical results support the experimental crossed molecular beams observations of vinylacetylene being the major product of the C$_2$H + C$_2$H$_4$ reaction and the fact that CH$_2$CHCCH is formed via a tight transition state with an exit barrier of 5−6 kcal/mol and also confirm that vinylacetylene can be produced from C$_2$H + C$_2$H$_4$ under low temperature conditions of Titan's atmosphere. The prevailing mechanism for the C$_2$H$_3$ + C$_2$H$_2$ reaction starts from the initial formation of different n-C$_4$H$_5$ conformers occurring with significant entrance barriers of ∼6 kcal/mol. The n-C$_4$H$_5$ isomers reside 35−38 kcal/mol lower in energy than C$_2$H$_3$ + C$_2$H$_2$ and can rapidly rearrange to one another overcoming relatively low barriers of 3−5 kcal/mol. H loss from the n-C$_4$H$_5$ species then gives the vinylacetylene product via exit barriers of ∼6 kcal/mol with the corresponding transition states lying 1.2−1.6 kcal/mol above the C$_2$H$_3$ + C$_2$H$_2$ reactants. Since the C$_2$H$_3$ + C$_2$H$_2$ reaction is hindered by relatively high entrance barriers, it is not expected to be important in Titan's atmospheric environments but can produce n-C$_4$H$_5$ or vinylacetylene under high temperature and pressure combustion conditions.
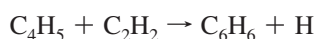
1. Introduction

Unraveling the mechanism of the formation of polycyclic aromatic hydrocarbons (PAH) and their hydrogen-deficient precursors through a set of elementary reactions of small hydrocarbon (HC) radicals with unsaturated HC molecules has been the subject of extensive experimental and theoretical studies,[1−9] which are of principal importance not only for combustion chemistry but also for better understanding the chemistry of the interstellar medium and planetary atmospheres, and in particular that of a Saturn's moon Titan. Titan attracts extraordinary research interest due to its famous haze layers—colored layers containing complex organic molecules, which are located in the stratosphere and absorb solar irradiation preventing Titan's atmosphere from heating up and, thus, being one of the reasons of its very low temperature of around 90 K. Such unique physical conditions allowed freezing the physical−chemical state of Titan at the early stage of its existence, making the whole moon an outstanding example of an "astro-physical−chemical museum" of the Solar System.

In Titan, molecular nitrogen and methane are the main constituents of the atmosphere followed by hydrogen, nitrogen-bearing molecules, and hydrocarbons. The studies of Titan's atmosphere based on the results of Huygens, Cassini, and Voyager I and II missions as well as ground and space astrochemical observations confirmed the presence of trace amounts (few parts per billion) of unsaturated HC molecules such as ethylene, acetylene, diacetylene, and benzene.[10,11] Accordingly, small HC radicals may be considered as products of photoinduced dissociation of these molecules (for example, the ethynyl radical C$_2$H is the product of the acetylene photolysis) and as intermediates in reactions of small HC radicals with unsaturated HC molecules. One should not be confused by small atmospheric concentrations of unsaturated HC on Titan, as they serve as the key intermediates in the formation and growth of large and complex organic species including PAH, playing an important role in Titan's haze layer chemistry.

Among many HC radicals that are likely to be present in Titan's atmosphere, C$_2$H is one of the most prominent species in context of the growth of larger organic molecules because of its very high reactivity and thus the possibility to react with

---

[†] Part of the special section "Chemistry: Titan Atmosphere".

unsaturated HC with no entrance barrier under Titan's low temperature conditions, resulting in the formation of unsaturated HC as well as other HC radicals involved in further elementary reactions to produce long polyyne chains and PAH, such as for example

$$C_2H + C_2H_2 \rightarrow C_4H_3 \rightarrow C_4H_2 + H$$

$$C_2H + C_4H_2 \rightarrow C_6H_3 \rightarrow C_6H_2 + H$$

$$C_4H_3 + C_2H_2 \rightarrow C_6H_5$$

$$C_6H_5 + nC_2H_2 \rightarrow PAHs$$

$$C_2H + C_2H_4 \rightarrow C_4H_5 \rightarrow C_4H_4 + H$$

$$C_4H_5 + C_2H_2 \rightarrow C_6H_6 + H$$

$$C_6H_6 + nC_2H \rightarrow PAHs$$

The present paper continues systematic theoretical studies of potential energy surfaces (PES), mechanism, and kinetics of the reactions of C_2H with unsaturated HC performed in our group.[5,12] In particular, we consider $C_2H + C_2H_4$ taking place on the C_4H_5 PES. This reaction is of significance because it may represent a viable route to the formation of C_4H_4 isomers under the conditions prevalent in Titan's atmosphere. Also, our theoretical investigation accompanies and complements the experimental crossed molecular beams study of the reaction dynamics of ethynyl radicals with deuterated ethylene.[13]

Clear knowledge of the global PES of C_4H_5 is of critical importance for unraveling the reaction mechanism, kinetics, and dynamics. Numerous theoretical works have been devoted to studying this surface and the properties of C_4H_5. For instance, Parker and Cooksy[14,15] reported results of extensive UHF, B3LYP, MP2, CISD, QCISD, and MCSCF computations on structures and energies of a number of low-energy C_4H_5 structures, including four n-C_4H_5 isomers HCCHCHCH$_2$, i-C_4H_5 H$_2$CCCHCH$_2$, cyclic c-C_4H_5 −H$_2$CCHCHCH−, H$_3$CCCCH$_2$, H$_3$CCHCCH, H$_2$CCH$_2$CCH, as well as their conformers being both local minima and saddle points on the PES. Nguyen et al.[16] studied a segment of the C_4H_5 PES related to the C(^{3}P) + allyl reaction and predicted vinylacetylene, H$_2$CCHCCH + H and $C_2H_3 + C_2H_2$ to be the major products. Wheeler et al.[17] investigated isomeric energy differences between i- and n-C_4H_5 isomers at the ROCCSD(T)/TZ(2d1f,2p1d) level. Hansen et al.[18] conducted quantitative identification of C_4H_5 isomers in fuel-rich allene, propyne, cyclopentene, and benzene flames, combining molecular-beam mass spectrometry and tunable vacuum-ultraviolet synchrotron radiation with B3LYP/6-311++G(d,p) and QCISD(T) calculations.

While many works on C_4H_5 isomers can be found in the literature, to the best of our knowledge, an exhaustive study of the global C_4H_5 PES at a high theoretical level providing chemical accuracy for the energetics and molecular parameters of intermediates and transition states has not yet been reported. The potential energy profiles for the considered reactions

$$C_2H + C_2H_4 \rightarrow C_4H_5$$

$$\rightarrow C_4H_4 + H$$
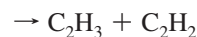
$$\rightarrow C_2H_3 + C_2H_2$$

are not available in the literature either, except for a very recent study by Woon and Park[19] who investigated several pathways leading from the reactants to vinylacetylene + H and $C_2H_3 + C_2H_2$ at the B3LYP/6-31+G** level. Also, two theoretical papers were devoted to the reverse $C_2H_3 + C_2H_2$ reaction. Wang and Frenklach[20] computed rate coefficients for $C_2H_3 + C_2H_2$ $\rightarrow C_4H_4 + H$ combining semiempirical AM1 calculations with RRKM kinetics studies, whereas Miller et al.[21] substantially extended this work and considered four $C_2H_3 + C_2H_2$ reaction channels, three of which lead to n-C_4H_5, i-C_4H_5, and c-C_4H_5 isomers and the fourth results in the formation of $C_4H_4 + H$. Miller et al.[21] employed DFT-B3LYP and G2-type methods to construct the appropriate portion of the C_4H_5 PES and RRKM theory to compute microcanonical rate constants and to solve master equations to estimate thermal rate coefficients and product distribution as a function of temperature and pressure.

In order to predict the outcome of chemical reactions accessing the C_4H_5 surface, we need to evaluate accurate energies of various C_4H_5 species since they can dramatically affect calculations of rate constants and product branching ratios. To achieve this goal, here we first carry out a study of the global C_4H_5 PES using DFT computations with further refinement of energies employing the chemically accurate CCSD(T) method. Our second goal is to construct all conceivable isomerization and dissociation pathways of the C_4H_5 species. Finally, we calculate rate constants and product branching ratios in order to analyze product distributions for the $C_2H + C_2H_4$ and $C_2H_3 + C_2H_3$ reactions. The kinetic calculations are performed under collisionless conditions, except the initial single collision between the reactants, and thus, rate constants and branching ratios are computed as functions of collision energy rather than temperature and pressure, making possible a direct comparison of our theoretical results with experimental observations from the crossed molecular beam experiments discussed in another paper in this issue.[13] Noteworthy, the conditions in Titan's atmosphere differ from single-collision conditions of crossed molecular beams experiments, as the pressure of nitrogen bath gas in the stratospheric region, where the $C_2H + C_2H_4$ reaction can occur, is in the range from 1×10^{-6} to 1 mbar. This may result in collisional stabilization of C_4H_5 intermediates, which is neglected in the present study. Woon and Park[19] have shown that such stabilization can be noticeable at pressures above 0.1 mbar at 50 K, above 1 mbar at 100 K, and even at higher pressures for higher temperatures. Since Titan's relevant temperature range is 90−200 K, we do not expect the collisional stabilization effects to be significant and limit the present consideration to the single-collision conditions.

2. Computational Methods

The geometries of the reactants, products, various isomers of C_4H_5, and transition states for isomerization and dissociation have been optimized by employing the hybrid density functional B3LYP method[22,23] with the 6-311G(d,p) set.[24] Vibrational frequencies, calculated at the same level, were used for characterization of the stationary points and zero-point energy corrections (ZPE). To obtain more accurate energies for all the species, we used the coupled cluster RCCSD(T)[25] calculations
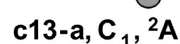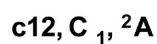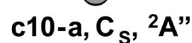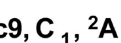
c1, C$_S$, ^{2}A'   **c2, C$_S$, ^{2}A''**   **c3, C$_S$, ^{2}A''**

c4-cis, C$_S$, ^{2}A'   **c4-trans, C$_S$, ^{2}A'**   **c5-cis, C$_1$, ^{2}A**

c5-trans, C$_1$, ^{2}A   **c6-a, C$_1$, ^{2}A**   **c6-b, C$_S$, ^{2}A'**

c7, C$_S$, ^{2}A''   **c8, C$_1$, ^{2}A**   **c9, C$_1$, ^{2}A**

c10-a, C$_S$, ^{2}A''   **c10-b, C$_1$, ^{2}A**   **c11, C$_S$, ^{2}A''**

c12, C$_1$, ^{2}A   **c13-a, C$_1$, ^{2}A**   **c13-b, C$_1$, ^{2}A**
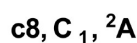
Figure 1. Part 1 of 4.

Figure 1. Part 2 of 4.
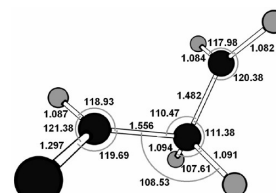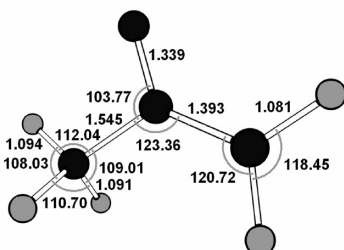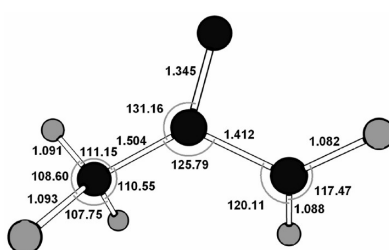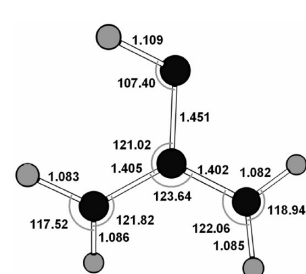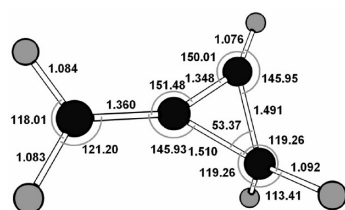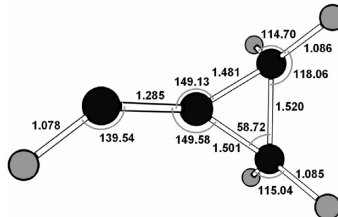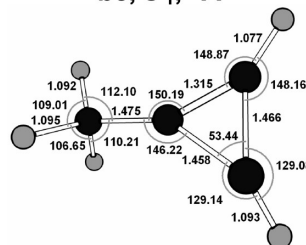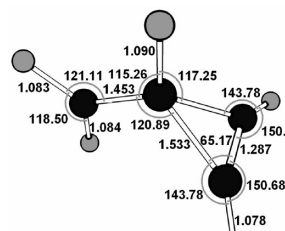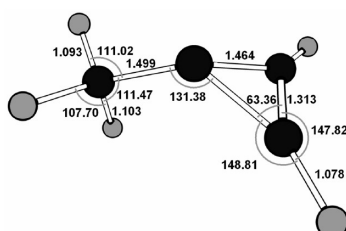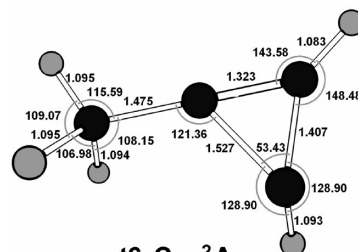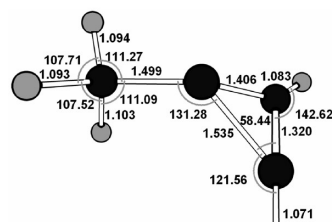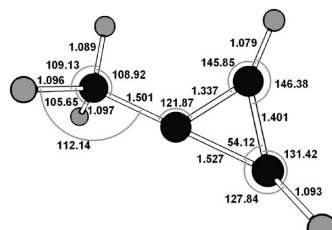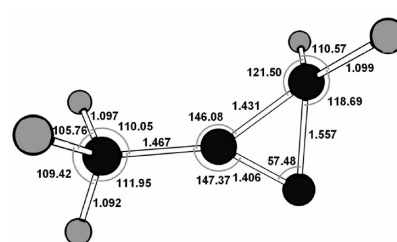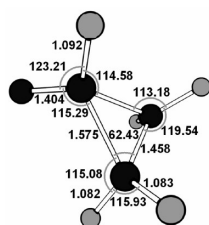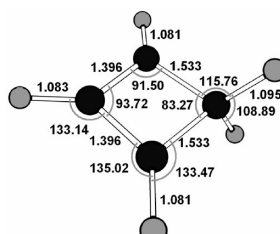
Figure 1. Part 3 of 4.

Figure 1. Part 4 of 4. Optimized geometries (bond lengths (Å) and bond angles (deg)) of various C₄H₅ local minima and possible products. Symmetry point groups and electronic states are also shown.

with the cc-pV(D,T,Q)Z basis sets.[26] The single-reference CCSD(T) method appeared to be appropriate for the C₄H₅ system, because T1 diagnostics values for all relevant intermediates and transitions states were in the range of 0.01–0.02 and hence multireference effects beyond the CCSD(T) treatment are not expected to be important. The GAUSSIAN 98[27] and MOLPRO 2002[28] programs were employed for the calculations.

We used the Rice–Ramsperger–Kassel–Marcus (RRKM) theory for computations of rate constants of individual reaction steps.[29] Rate constant $k(E)$ at an internal energy E for a unimolecular reaction A* → A# → P can be expressed as

$$k(E) = \frac{\sigma W^{\ddagger}(E - E^{\ddagger})}{h\rho(E)}$$

where σ is the reaction path degeneracy, h is Planck's constant, $W^{\ddagger}(E - E^{\ddagger})$ denotes the total number of states for the transition state (activated complex) A# with a barrier $E^{\#}$, $\rho(E)$ represents the density of states of the energized reactant molecule A*, and P is the product or products. Here, E is the internal vibrational energy of C₄H₅ species acquired due to their chemical activation in the C₂H + C₂H₄ reaction. This energy includes the relative energy of C₂H + C₂H₄ with respect to the C₄H₅ isomer being considered plus the reaction collision energy assuming that the major fraction of the latter is converted to the internal vibrational energy of C₄H₅. This approach for evaluation of E is valid for single-collision conditions of crossed molecular beams experiments where the C₄H₅ species formed in the reaction cannot dissipate their internal energy by collisions. The total number of states and density of states were computed using the direct

count method.[30] We used harmonic approximation to calculate the total number and density of states.

Assuming single-collision conditions, master equations for unimolecular reactions can be expressed as

$$\frac{d[C]_i}{dt} = \sum k_n[C]_j - \sum k_m[C]_i$$

where $[C]_i$ and $[C]_j$ are concentrations of various intermediates or products and k_n and k_m are microcanonical rate constants computed using the RRKM theory. Only a single total-energy level was considered throughout, as for single-collision crossed-beam conditions. In such a case, rate constants of different unimolecular reaction steps are independent of each other, but relative product yields can be determined from the solut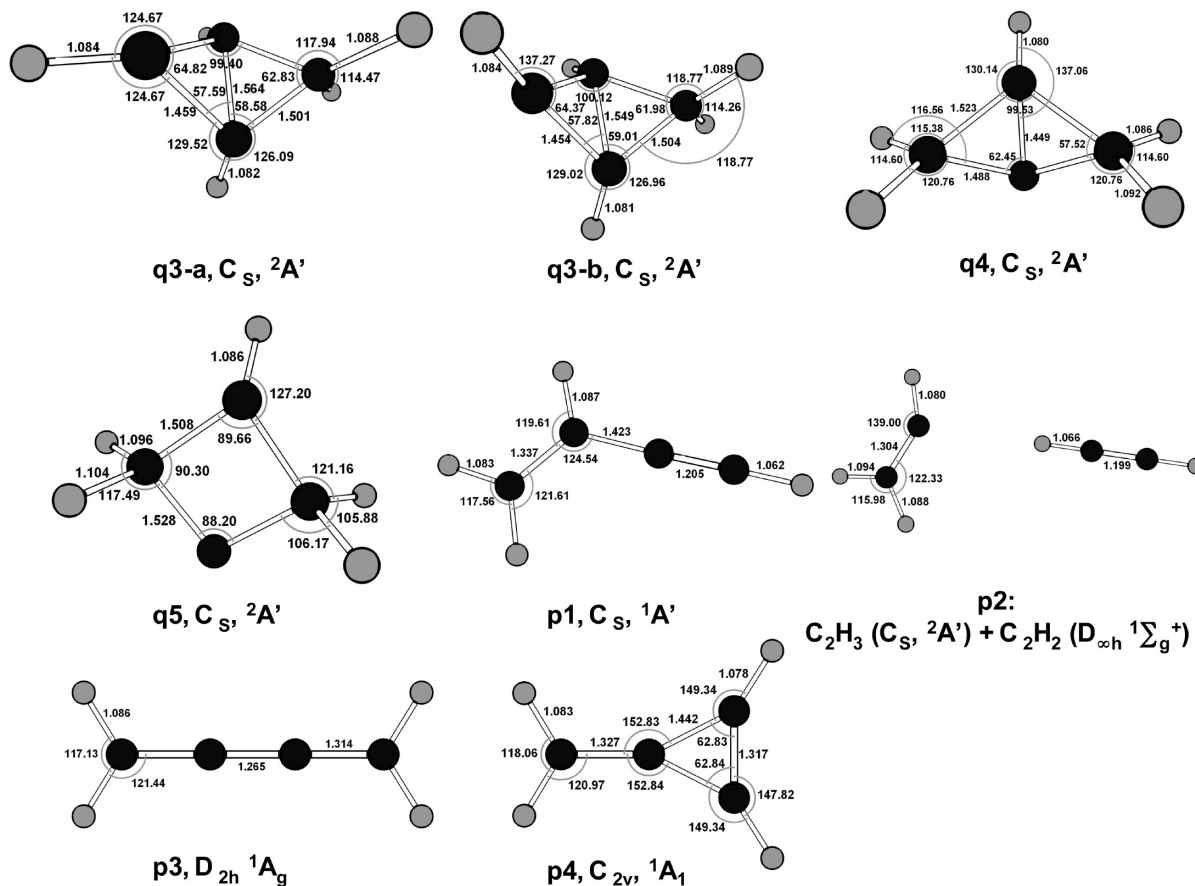ion of the system of coupled master equations. The fourth-order Runge–Kutta method[31] was employed to solve the master equations and to obtain numerical solutions for the concentrations of various products versus time. The concentrations at the times when they have converged were used for calculations of the product branching ratios.

It should be noted that the bimolecular rate constant for the initial reaction step of C₂H addition to C₂H₄ was not considered here. We simply assume that this step can take place to produce chemically activated C₄H₅ adducts, which then undergo unimolecular isomerization and dissociation reactions, and then analyze product branching ratios for these unimolecular reactions.

3. Results and Discussion

3.1. The C₂H + C₂H₄ Reaction. To construct the global potential surface of C₄H₅, numerous structures consisting of four

11118 *J. Phys. Chem. A, Vol. 113, No. 42, 2009*

Krishtal et al.

carbon and five hydrogen atoms have been examined at the B3LYP/6-311G(d,p) level of theory. Figure 1 shows optimized structures of all stable C_4H_5 isomers, which have been found in our optimizations, and Table 1 presents their relative energies as calculated using the B3LYP/6-311G(d,p) and CCSD(T)/cc-pVQZ//B3LYP/6-311G(d,p) + ZPE(B3LYP/6-311G(d,p)) computational methods.

The classification of isomers in Figure 1 reflects their characteristic features attributed to one of five possible topological patterns that can be formed by four C atoms: isomers denoted with "c" (c-isomers), chains made of four carbons; isomers denoted with "b"(b-isomers), branching structures with the central C atom with three CC bonds and three C atoms forming one CC bond with the central C atom; isomers denoted with "t" (t-isomers), three-member rings with an out-of-ring CC bond; and isomers denoted with "q" (q-isomers), four-member rings and bicyclic structures consisted of two three-member rings fused together.

Of the total number of 58 recognized isomers, 39, 3, 10, and 6 species belong to the c-, b-, t-, and q-types, respectively; optical isomers with identical structural composition are designated as a single isomer. For each isomer, bond lengths, bond angles, symmetry group, and electronic state are shown in Figure 1. Below, each of four groups of isomers is considered in some detail.

Figure 1 and Table 1 also contain the optimized structures and energies of possible products denoted with the letter "p".

Chain Isomers. The most stable of chain isomers (here and below we will rely on relative CCSD(T)/cc-pVQZ energies with ZPE corrections with respect to the $C_2H + C_2H_4$ reactants) is H_3CCCCH_2 c1 ($\Delta E_{CCSD(T)} = -72.5$ kcal/mol). It is also the most stable isomer on the global C_4H_5 PES, which agrees with the conclusions of the previous works.[15,32,33] In terms of resonance structures, c1 can be described as a mixture of $H_3C-C\equiv C-C^\bullet H_2$ (2-butyn-1-yl) and $H_3C-C^\bullet=C=CH_2$ (1,2-butadien-3-yl). The next in the order of stability chain isomer and the second most stable isomer found in the present study is $H_2CCHCCH_2$ c2 (i-C_4H_5) with $\Delta E_{CCSD(T)} = -70.0$ kcal/mol, which is 2.5 kcal/mol higher in energy than c1. Apparently, it is resonance stabilized and can be described as a mixture of $H_2C=CH-C^\bullet=CH_2$ (1,3-butadien-3-yl) and $H_2C^\bullet-CH=C=CH_2$ (2,3-butadien-1-yl). The third most stable chain isomer (and the third overall) $H_3CCHCHCH$ c3 is only 0.2 kcal/mol higher in energy than c2. It also possesses two resonance structures, $H_3C-C^\bullet H-C\equiv CH$ (1-butyn-3-yl) and $H_3C-CH=C=C^\bullet H$ (1,2-butadien-1-yl). Parker and Cooksy[15] discussed in detail different conformers of c1, c2, and c3, being both minima and saddle points on the global C_4H_5 PES. Since those conformers have only minor differences in energy and geometry and their isomerization is not expected to affect the overall reaction kinetics, here we limit ourselves only to representative minimum energy structures and refer the reader to the earlier work.[15]

Next are four $HC^\bullet=CH-CH=CH_2$ 1,3-butadien-1-yl conformers, c4-cis, c4-trans, c5-cis, and c5-trans. They represent different conformations of n-C_4H_5, where the arrangement of the carbon chain is trans and cis in c4 and c5, respectively. These isomers, which have been extensively studied by Parker and Cooksy,[14] are not resonance stabilized and lie 12.3, 12.8, 14.9, and 15.4 kcal/mol higher in energy than c1, respectively. Isomer $H_2C^\bullet-CH_2-C\equiv CH$ c6 (1-butyn-4-yl), which can serve as an initial adduct in the $C_2H + C_2H_4$ reaction, is not resonance stabilized and has two minimum energy conformers c6-a and c6-b that differ in the torsion angle of the terminal CH_2 group

TABLE 1: Total (hartree, E_{B3LYP}) and Relative (kcal/mol, with respect to $C_2H + C_2H_4$) Energies of C_4H_5 and C_4H_4 Isomers from B3LYP/6-311G(d,p) (ΔE_{B3LYP}) and CCSD(T)/cc-pVQZ//B3LYP/6-311G(d,p) + ZPE ($\Delta E_{CCSD(T)}$) Calculations

species	E_{B3LYP}	ΔE_{B3LYP}	$\Delta E_{CCSD(T)}$
c1	−155.37309	−81.4	−72.5
c2	−155.37085	−80.0	−70.1
c3	−155.36733	−77.7	−69.8
c4-cis	−155.34991	−66.8	−60.2
c4-trans	−155.34895	−66.2	−59.6
c5-cis	−155.34490	−63.7	−57.6
c5-trans	−155.34416	−63.2	−57.1
c6-a	−155.34004	−60.6	−56.9
c6-b	−155.33932	−60.2	−56.1
c7	−155.30567	−39.1	−33.1
c8	−155.30030	−35.7	−30.5
c9	−155.30056	−35.8	−30.0
c10-a	−155.28957	−28.9	−22.5
c10-b	−155.28737	−27.6	−20.3
c11	−155.28980	−29.1	−23.0
c12	−155.29216	−30.6	−21.3
c13-a	−155.26347	−12.6	−10.4
c13-b	−155.26304	−12.3	−10.0
c14	−155.26252	−12.0	−7.3
c15	−155.25978	−10.3	−5.8
c16-cis	−155.24791	−2.8	4.2
c16-trans	−155.24976	−4.0	4.7
c17-a	−155.24133	1.3	6.9
c17-b	−155.24738	−2.5	12.3
c18	−155.13970	65.1	73.9
c19-cis−cis	−155.22766	9.9	14.8
c19-trans−cis	−155.23022	8.3	13.5
c19-trans−trans	−155.23776	3.6	7.5
c20	−155.22567	11.2	17.7
c21	−155.13967	65.1	135.4
c22-a	−155.14731	60.3	103.6
c22-b	−155.14206	63.6	72.2
c22-c	−155.14206	63.6	72.2
c23-a	−155.22540	11.3	18.4
c23-b	−155.22381	12.3	16.5
c23-c	−155.22596	11.0	17.5
c24	−155.14132	64.1	71.1
c25	−155.21798	16.0	21.6
c26	−155.26585	−14.1	−10.0
b1	−155.28783	−27.9	−21.8
b2	−155.28588	−26.6	−20.8
b3	−155.26521	−13.7	−8.6
t1	−155.34236	−62.1	−53.7
t2	−155.32432	−50.8	−44.0
t3	−155.32021	−48.2	−41.9
t4	−155.31585	−45.4	−40.9
t5	−155.31498	−44.9	−39.0
t6	−155.30322	−37.5	−31.5
t7	−155.29944	−35.1	−29.8
t8	−155.29595	−33.0	−26.9
t9	−155.26712	−14.9	−16.8
t10	−155.26749	−15.1	−9.6
q1	−155.36174	−74.2	−68.6
q2	−155.32827	−53.2	−48.2
q3-a	−155.31985	−47.9	−43.7
q3-b	−155.31012	−41.8	−37.6
q4	−155.30062	−35.9	−31.0
q5	−155.24099	1.5	6.0
p1 + H	−155.28295	−24.8	−26.6
p2	−155.28117	−23.7	−22.2
p3 + H	−155.27733	−21.3	−18.8
p4 + H	−155.24415	−0.4	−2.9

relative to the single CC bond, as described in detail by Parker and Cooksy,[15] and lie 15.9 and 16.4 kcal/mol higher in energy than c1. It should be noted that the rotational conformers of c6
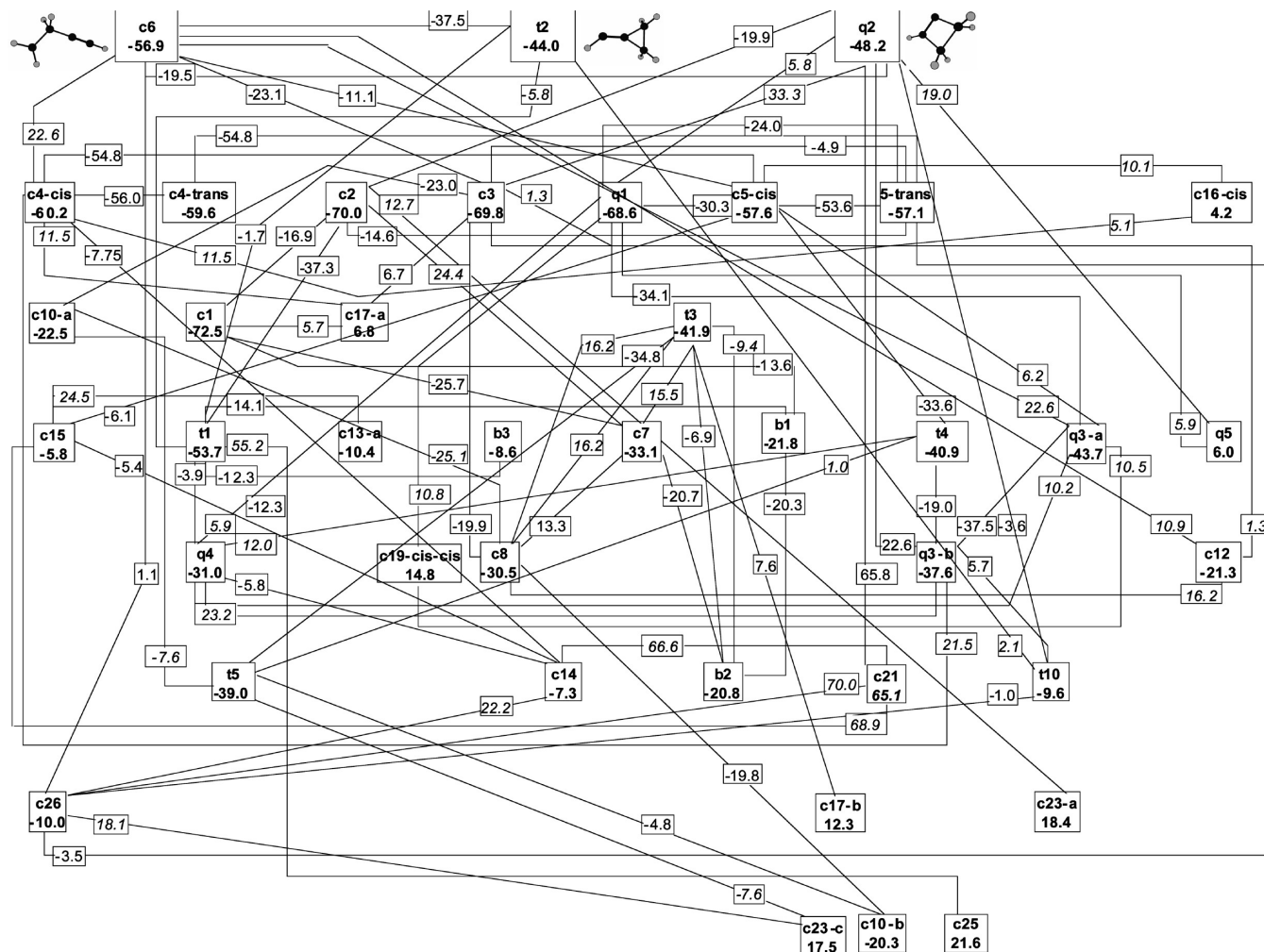
Figure 2. Full graph of possible isomerization and dissociation pathways on the PES of the C_4H_5 radical. Relative energies (in kcal/mol) are taken from CCSD(T)/cc-pVQZ//B3LYP/6-311G(d,p)+ZPE calculations. Energies of transition states taken from B3LYP/6-311G(d,p) are shown in italic.

differ in energy slightly more than the cis- and trans-conformers of c4 and c5 (0.8 kcal/mol versus 0.6 and 0.4 kcal/mol, respectively). The rest of chain isomers lie at least 39.4 kcal/mol higher in energy than c1.

There are a number of isomers (c7, c8, c9, and the c19 group) that have been included in this class despite the fact that they allow for an ambiguous classification because their structures are intermediate between strongly bend chains and three-member rings with nearly open ring conformations. Such isomers are characterized by a prolonged (~1.6 Å) CC bond connecting one of carbon atoms in the three-member ring with the carbon forming an out-of-ring CC bond. The reason for moving them into the "c" category is to distinguish them from the corresponding "pure" three-member ring isomers, which visually look similar but significantly differ in bond lengths/angles and energies. Here, such "improper" three-member rings are included to the chain class if the length of the longest CC bond in the ring is equal or exceeds 1.6 Å.

Branching Isomers. We were able to identify three branching isomers, b1, b2, and b3, which are 50.7, 51.7, and 63.9 kcal/mol higher in energy than the most stable c1 species.

Three-Member Rings. We found 10 isomers consisted of a three-member ring and an out-of-ring CC bond. The most stable of them, t1, lies 18.8 kcal/mol above c1. The rest reside 28.5−62.9 kcal/mol higher in energy than c1. Notably, the $HCCCH_2CH_2$ t2 isomer is a possible initial adduct in the barrierless $C_2H + C_2H_4$ reaction.

Four-Member Rings and Bicyclic Structures. Six isomers were attributed to the q-type according to our classification. The most stable of them, $-CH_2CHCHCH-$ q1 falls into the category of very stable C_4H_5 isomers ($\Delta E_{CCSD(T)} = -68.6$ kcal/mol) and is stabilized by having two resonance structures: $-CH_2-C^{\bullet}H-CH=CH-$ and $-CH_2-CH=CH-C^{\bullet}H-$ (cyclobut-1-en-3-yl and cyclobut-2-en-1-yl). The remaining isomers of this type are presented by q2, q3-a, q3-b, and q4, which are 24.3, 28.8, 37.6, and 41.5 kcal/mol higher in energy than c1, and by a high energy q5 isomer, 78.5 kcal/mol above c1. The most important q-isomer in our study is four-member ring q2, $-CH=C^{\bullet}-CH_2-CH_2-$ (cyclobut-1-en-2-yl), which is one of three possible initial adducts in the $C_2H + C_2H_4$ reaction along with acyclic c6 and three-member ring t2.

The full graph of possible isomerization pathways on the global PES of C_4H_5 is shown in Figure 2 (possible dissociation pathways are not shown for simplicity). Since all isomers as well as pathways containing transition states with positive relative energies with respect to $C_2H + C_2H_4$ are not likely to contribute to the most favorable reaction channels and hence are not of interest for calculations of rate constants and product branching ratios, we constructed a simplified graph by removing them from the full graph. We have also excluded all isomers with negative relative energies that can only be approached via transition states with positive relative energies. The new graph containing only isomers and pathways with negative relative energies and also all energetically favorable dissociation
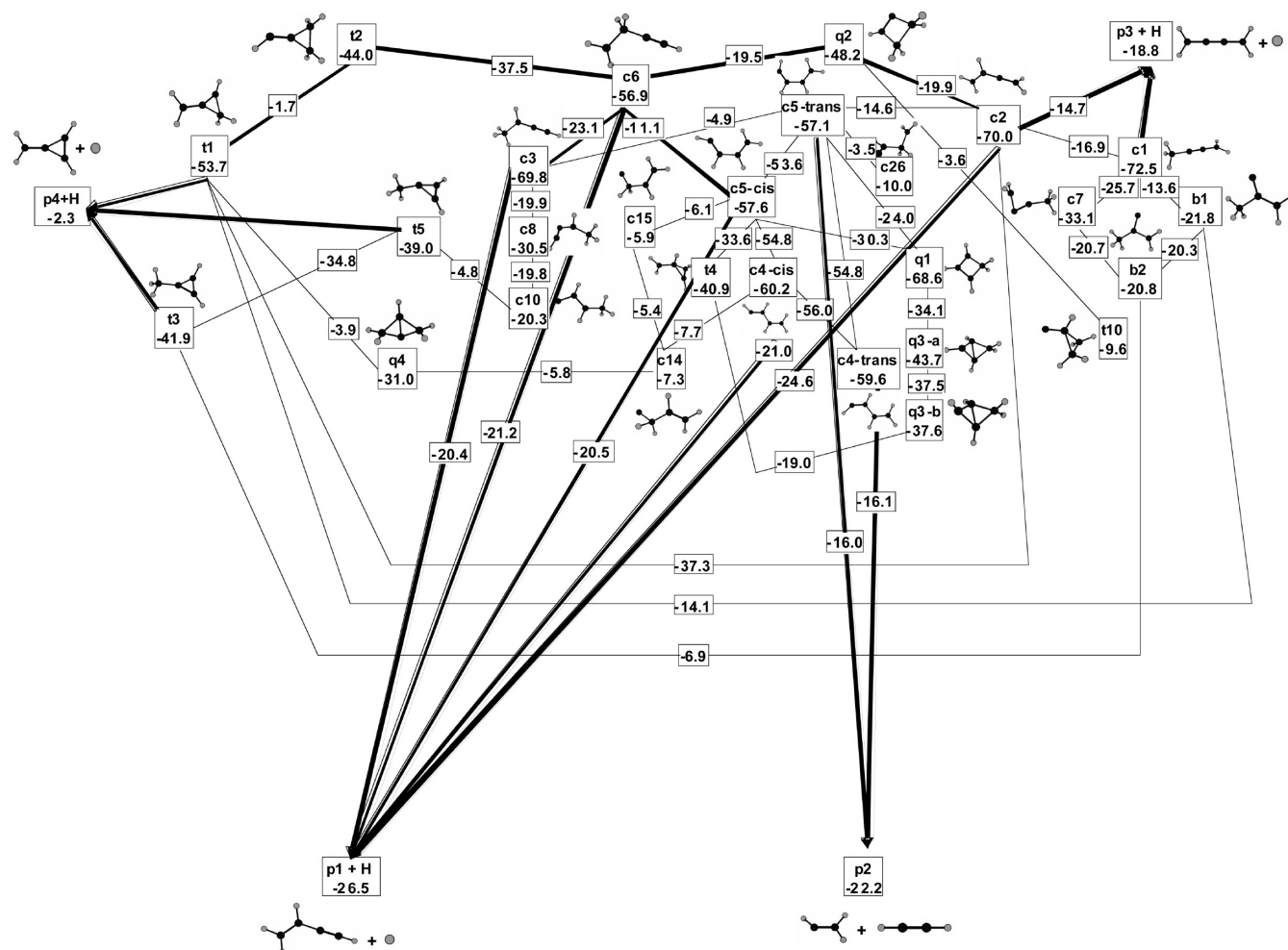
Figure 3. Overall kinetic scheme of the $C_2H + C_2H_4$ reaction used in calculations of product branching ratios. Relative energies are taken from CCSD(T)/cc-pVQZ//B3LYP/6-311G(d,p)+ZPE calculations.

pathways (where both transition states and corresponding products have negative relative energies) is illustrated in Figure 3. Thus, the graph in Figure 3 represents the kinetics scheme needed for studying the $C_2H + C_2H_4$ reaction.

Reaction Channels for the $C_2H + C_2H_4$ Reaction. Due to a high reactivity of the C_2H radical, the $C_2H + C_2H_4$ reaction has three possible entrance channels which can proceed through barrierless C_2H addition to ethylene to form one chain and two cyclic initial adducts; c6 is formed by simple C_2H addition to one of the carbon atoms of C_2H_4, whereas the three- and four-member ring structures t2 and q2 are produced by C_2H cyclo additions to the double C=C bond in the end-on and side-on manner, respectively. Here and below no difference is made between c6-a and c6-b conformers; rather, both of them are denoted as a single c6 isomer. While all three channels are theoretically accessible, the formation of the acyclic initial adduct c6 is likely to be the dominant process here. To confirm this quantitatively, dynamics calculations need to be carried out; however, there is indirect evidence supporting the preference of the $C_2H + C_2H_4 \rightarrow$ c6 channel. First, c6 is the most stable isomer among the three initial adducts. Also, if the initial channel were the formation of the three-member ring t2, then further reaction step would anyway proceed through ring-opening to form the chain isomer c6 rather than through a 1,3-H shift in t2 to form t1 because of a very high barrier for the t2-t1 step, 42.3 kcal/mol as compared to 6.5 kcal/mol for the barrier height for t2-c6. Second, our attempts to locate transition states for the $C_2H + C_2H_4 \rightarrow$ t2 and $C_2H + C_2H_4 \rightarrow$ q2 channels were

unsuccessful, and finally, in our recent study of the $C_2H + C_4H_2$ reaction,[12a] we concluded that the dominant entrance channel is barrierless addition of C_2H to a carbon atom of C_2H_2 to form an acyclic initial adduct C_6H_3. A similarity of these two reactions allows us to suggest that the same type of entrance channel with formation of the acyclic isomer c6 should be favorable for $C_2H + C_2H_4$. Nevertheless, for more complete description of possible isomerization and dissociation channels on the global C_4H_5 PES, we will consider below all three channels as theoretically feasible, but the dominance of the $C_2H + C_2H_4 \rightarrow$ c6 channel will be taken into account in our kinetics calculations.

According to the energetics data in Table 1 and the kinetic scheme in Figure 3, four possible products can be achieved in the $C_2H + C_2H_4$ reaction via numerous reaction channels. These products include three C_4H_4 isomers plus H (two chains and one three-member ring) as well as $C_2H_3 + C_2H_2$. In terms of the order of stability, they are (1) $H_2CCHCCH$, p1 (vinylacetylene) + H, (2) $C_2H_3 + C_2H_2$, p2 (vinyl radical + acetylene), (3) H_2CCCCH_2, p3 (butatriene) + H, and (4) $H_2CCCHCH_2$, p4 (methylenecyclopropene) + H. In our earlier work,[34] we showed that C_4H_4 isomers, identified here as the products of the $C_2H + C_2H_4$ reaction, are the most stable species on the global singlet C_4H_4 PES. Since our interest is limited to the above three C_4H_4 isomers and a detailed discussion on the C_4H_4 PES can be found elsewhere,[34] we do not consider other C_4H_4 isomers in the present study. Also, we were not able to find any reasonably low energy pathway leading to the $C_4H_3 + H_2$ products.

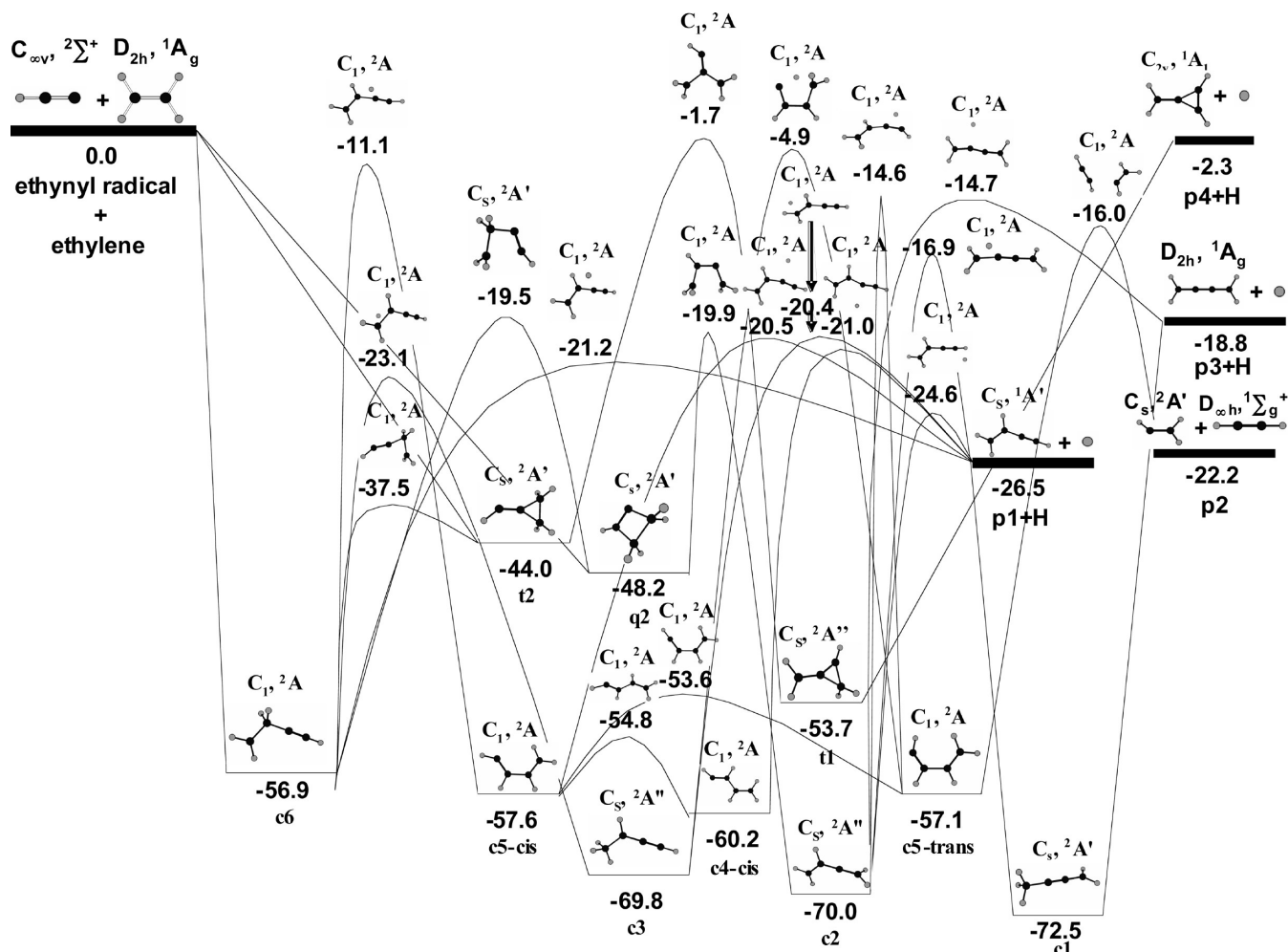**Figure 4.** Potential energy diagram for the most important channels of the C$_2$H + C$_2$H$_4$ reaction.

Figure 4 shows the most important channels extracted from the overall kinetic scheme, which result in dissociation of C$_4$H$_5$ intermediates to form the p1−p4 products. They are discussed in detail below.

Formation of Vinylacetylene. The most straightforward one-step pathway to form vinylacetylene is a direct H elimination from the initial adduct c6 occurring with an exit barrier of 5.3 kcal/mol (channel c6−p1). There are also four possible two-step pathways resulting in the formation of vinylacetylene, namely: (1) 1,2-H shift in the initial adduct c6 to form c3 followed by H loss from the CH$_3$ group of c3 taking place with an exit barrier of 6.1 kcal/mol (c6-c3-p1); (2) 1,2-H shift in the same isomer accompanied with a loss of linearity along the CCC axis to form c5-cis followed by H loss with an exit barrier of 6.0 kcal/mol (c6−c5-cis−p1); (3) cleavage of the H$_2$C−CH$_2$ bond in the initial adduct q2 to form c2 followed by H loss from one of the terminal CH$_2$ groups in c2 with an exit barrier of 1.9 kcal/mol (q2−c2−p1); (4) cleavage of one of the H$_2$C−C bonds in the initial adduct t2 to form c6 followed by H elimination from c6 (t2−c6−p1). Note that the H loss transition state from c3 in channel (2) could not be located using the B3LYP method as this process proceeds without an exit barrier within this level of theory. However, the transition state was found using Møller−Plesset second-order perturbation theory MP2/6-311G** geometry optimization and the existence of the barrier was confirmed by single-point CCSD(T)/cc-pVQZ calculations. Possible three-step pathways to p1 include (1) the c6−c5-cis rearrangement followed by isomerization of c5-cis

to c4-cis by internal rotation of a C$_2$H$_2$− fragment and then by H loss from c4-cis with an exit barrier of 5.5 kcal/mol (c6−c5-cis−c4-cis−p1); (2) isomerization of c6 via ring closure to q2 followed by merging into the q2−c2−p1 channel (c6−q2−c2−p1); (3) cleavage of one of the H$_2$C−C bonds in the initial adduct t2 followed by entering into the channels starting from the initial adduct c6 (t2−c6−c3−p1 and t2−c6−c5-cis−p1). Next, potential four-step routes incorporate (1) the c6−c3 isomerization followed by 1,3-H migration in c3 to form c5-trans, then transformation of c5-trans into c5-cis, and finally H loss from c5-cis (c6−c3−c5-trans−c5-cis−p1); (2) the q2−c2 rearrangement, then 1,2-H shift in c2 to form c5-trans followed by entering into either c6−p1 or c5-cis−p1 routes (q2−c2−c5-trans−c3−p1 and q2−c2−c5-trans−c5-cis−p1); (3) a combination of the channels t2−c6−c5-cis and c4-cis−p1 described above (t2−c6−c5-cis−c4-cis−p1).

There are also few theoretically feasible pathways with five and more steps; however, since all of them are combinations of the channels considered above with addition of a number of intermediate steps, we do not discuss them. The channels involving the 1,3-H migration at the c3−c5-trans stage in both directions, c6−c3−c5-trans−c5-cis−p1 and q2−c2−c5-trans−c3−p1 seem to be practically inaccessible due to a very high energy barrier for this process with the transition state located at −4.9 kcal/mol.

Formation of Vinyl Radical + Acetylene. According to Figure 3, C$_2$H$_3$ + C$_2$H$_2$ cannot be formed through one- or two-step mechanisms but can be produced via several three-step

routes, namely: (1) the c6−c3−c5-trans isomerization sequence followed by a cleavage of the HCCH−CHCH₂ bond in c5-trans with an exit barrier of 6.2 kcal/mol (c6−c3−c5-trans−p2); (2) the c6−c5-cis−c5-trans rearrangements followed by dissociation of c5-trans (c6−c5-cis−c5-trans−p2); and (3) q2−c2−c5-trans−p2. Also, numerous four-step channels to C₂H₃ + C₂H₂ include c6−q2−c2−c5-trans−p2, t2−c6−c3−c5-trans−p2 and t2−c6−c5-cis−c5-trans−p2, c6−c3−c5-trans−c4-trans−p2, c6−c5-cis−c5-trans−c4-trans−p2, q2−c2−c5-trans−c4-trans−p2, c6−c5-cis−c4-cis−c4-trans−p2, t2−t1−c2−c5-trans−p2, and c6−c5-cis−q1−c5-trans−p2. As was mentioned above, the channels containing the c3−c5-trans or c5-trans−c3 steps are virtually inaccessible since they involve the energetically unfavorable 1,3-H migration process. Therefore, the c6−c3−c5-trans−p2, t2−c6−c3−c5-trans−p2, and c6−c3−c5-trans−c4-trans−p2 routes are unlikely to occur and to lead to C₂H₃ + C₂H₂. The channel t2−t1−c2−c5-trans−p2 is mentioned only for completeness because the t2−t1 isomerization goes through a very high barrier, with the transition state residing at −1.7 kcal/mol, making this process improbable.

Formation of Butatriene. In contrast to the C₂H₃ + C₂H₃ products, the formation of butatriene p3 can be achieved through a two-step pathway, which starts from the initial four-member ring adduct q2, proceeds to c2, and completes by H loss from the CH group in c2 with an exit barrier of 4.1 kcal/mol (q2−c2−p3). Alternative channels include several three- and four-step pathways, namely: (1) starting from the q2−c2 rearrangement followed by 1,2-H shift in c2 to form the most stable isomer c1 and completed by H elimination from the CH₃ group in c1 proceeding without an exit barrier (q2−c2−c1−p3); (2) starting from the acyclic initial adduct c6 via c6−q2−c2 (c6−q2−c2−p3); (3) starting from the three-member ring initial adduct t2 via t2−t1−c2 (t2−t1−c2−p3); (4) t2−c6−q2−c2−p3; (5) t2−t1−c2−c1−p3; (5) t2−t1−b1−c1−p3; (6) c6−q2−c2−c1−p3; (7) c6−c3−c5-trans−c2−p3; and (8) c6−c5-cis−c5-trans−c2−p3. Again, it should be noted that the channels including the transformation of t2 into t1 through the 1,3-H shift, i.e., t2−t1−c2−p3, t2−t1−c2−c1−p3, and t2−t1−b1−c1−p3 are not likely to be accessible because of the very high barrier for the t2−t1 isomerization. This is also the case for the c6−c3−c5-trans−c2−p3 channel because of the energetically hindered c3−c5-trans step (see above).

Formation of Methylenecyclopropene. Methylenecyclopropene p4 is located only 2.4 kcal/mol lower in energy than C₂H + C₂H₄ and 24.1 kcal/mol above vinylacetylene and so it seems to be an unlikely product of the C₂H + C₂H₄ reaction. There are few channels though that may be purely theoretically considered as feasible routes approaching p4. For instance, according to the overall kinetic scheme in Figure 3, p4 can be achieved by three barrierless exit channels, namely: (1) H elimination from the CH₂ group of the three-member ring t1 isomer (t1−p4); (2) H elimination from the CH₃ group of the three-member ring t5 structure (t5−p4); and (3) H elimination from the CH₃ group of the three-member ring t3 intermediate (t3−p4). A two-step pathway starts from the initial cyclic adduct t2 and proceeds via t1 to p4 (t2−t1−p4). This channel is inaccessible in practice because of the very high barrier for the t2−t1 isomerization, thus also making the three-step c6−t2−t1−p4 and four-step q2−c6−t2−t1−p4 channels implausible. There exists one three-step channel, which energetically is more preferable that the above mechanisms as it does not include the t2−t1 step. It starts from the cyclic initial adduct q2, proceeds through q2−c2 with an isomerization barrier of 28.8 kcal/mol and then to t1 via ring closure in c2 with a barrier of

50.1 kcal/mol, and completes by H elimination via the exit step t1−p4 (q2−c2−t1−p4). The exit channels t5−p4 and t3−p4 and the rest of pathways involving t1−p4 are only reachable through five and more step mechanisms occurring with high barriers, making them completely inaccessible in practice.

Rate Constants and Product Branching Ratios. After the most important reaction channels considered above were analyzed, the following routes have been selected for kinetic studies by solving together coupled master equations: (1) c6−p1, this channel is the most straightforward pathway to directly produce p1 from the acyclic initial adduct c6; (2) c6−c3−p1, this channel represents an energetically favorable two-step pathway to form p1. (3) c6−c5-cis−p1, although the barrier for the c6−c5-cis step is almost twice as high as that for c6−c3, we have included this channel as an alternative two-step mechanism leading to p1; (4) q2−c2−p1, assuming q2 as the initial adduct in the C₂H + C₂H₄ reaction, this channel may also serve as an alternative for the formation of vinylacetylene through a four-member ring opening followed by H elimination; (5) c6−c5-cis−c5-trans−p2, the three-step mechanism seems to be the only plausible pathway to form C₂H₂ + C₂H₃, p2, in the C₂H + C₂H₄ reaction; (6) q2−c2−c5-trans−p2, this channel, which starts by ring opening in the four-member ring q2, is an alternative for the formation of p2 from the acyclic initial adduct c6 in the previous channel (5). (7) q2−c2−p3, this channel represents a two-step pathway to produce butatriene, p3; (8) c2−p1−p3, an alternative channel to form butatriene.

In our kinetic studies, we did not include any pathways resulting in the formation of methylenecyclopropylene, p4, for the following reasons. First, the dissociation channels leading to p4 can be approached either through very high energy barriers or via multistep pathways that are not competitive with the main production channels 1−8. Second, p4 itself resides only 2.3 kcal/mol below the reactants while the other products are respectively 26.5, 22.2, and 18.8 kcal/mol lower in energy than C₂H + C₂H₄.

The calculated rate constants for the unimolecular reaction steps illustrated in Figure 5 are collected in Table 2, and branching ratios for different product channels are presented in Table 3. The calculations were carried out assuming zero collision energy, i.e., zero internal energy in excess of the reactants zero-point level. One can see that vinylacetylene is a nearly exclusive reaction product, with ∼78% of the total yield produced directly from the initial adduct c6 and ∼21% formed via the c6−c3−p1 route. The contribution of the C₂H₃ + C₂H₂ products does not exceed 0.1% and butatriene can be produced only in miniscule amounts. These results appear to be very close to the relative yields computed for the C₂H + C₂D₄ reaction at the experimental collision energy of 20.6 kJ/mol (4.9 kcal/mol), which showed the deuterated vinylacetylene CD₂CDCCH as practically the only product with the relative yield of the c6−p1 and c6−c3−p1 channels being 76.7% and 21.8%.[13] The RRKM calculations clearly support the experimental observation that the reaction of ethynyl radical with ethylene produces vinylacetylene under single-collision conditions. It should be noted that the present results agree with those from the recent kinetic multiwell calculations by Woon and Park based on their B3LYP/6-31+G** PES.[19] They also found vinylacetylene + H as the dominant C₂H + C₂H₄ reaction product at low pressures at *T* = 50−300 K, with no C₂H₃ + C₂H₂ being produced, whereas the pathways to butatriene or methylenecyclopropene were not considered. In addition, Woon and Park[19] evaluated pressure effects and found that among C₄H₅ species, c3 can be stabilized
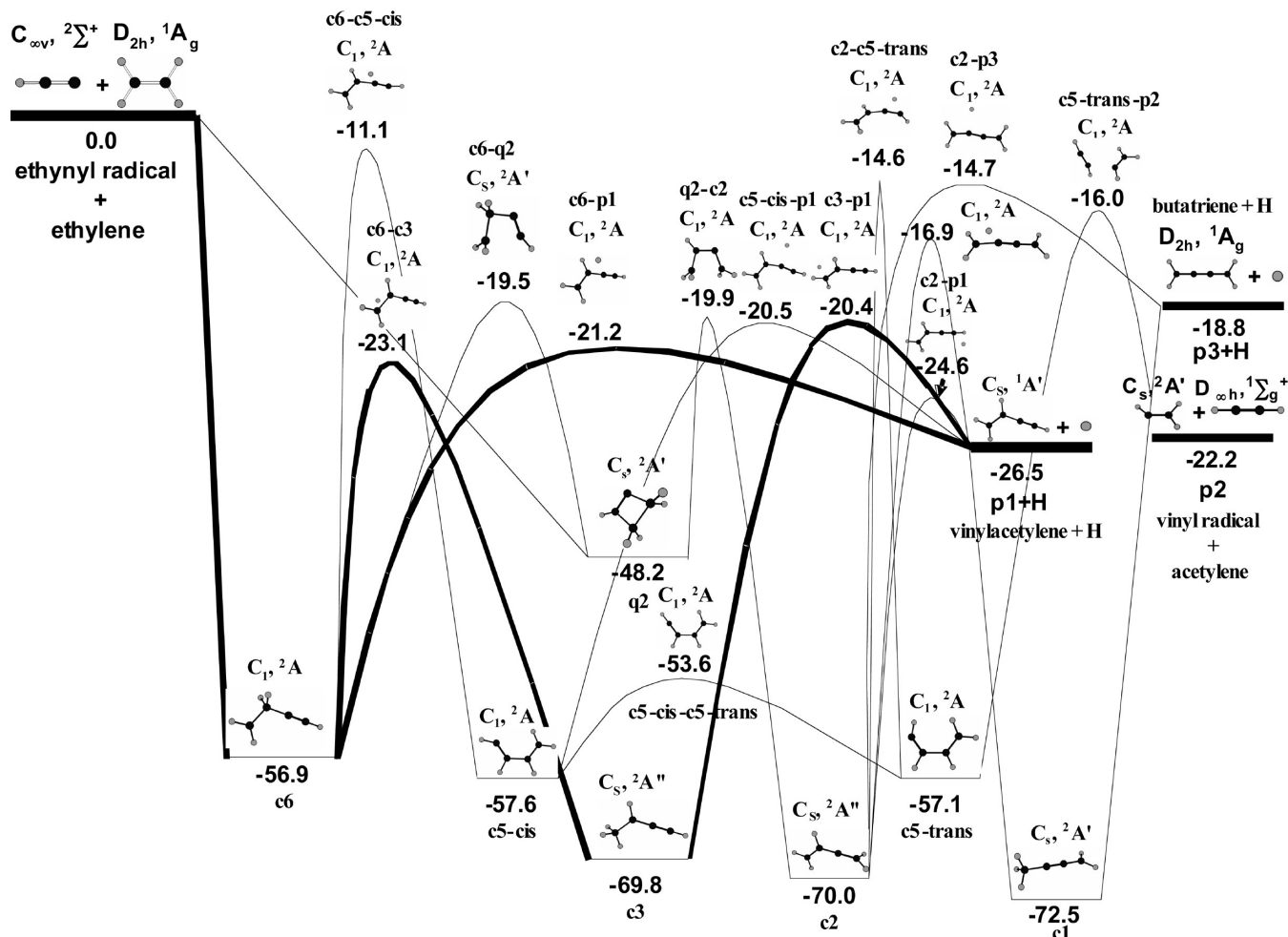
Figure 5. C_2H + C_2H_4 reaction channels used in calculations of rate constants and product branching ratios. The most important reaction routes are shown by bold lines.

TABLE 2: Microcanonical Rate Constants (s^{-1}) for Unimolecular Reaction Channels Used for Calculations of Product Branching Ratios[a]

channel	rate constant
k_1: c6 → q2	1.03×10^7
k_{-1}: q2 → c6	1.26×10^{10}
k_2: c6 → c3	3.62×10^8
k_{-2}: c3 → c6	8.94×10^7
k_3: c6 → c5-cis	9.29×10^5
k_{-3}: c5-cis → c6	2.23×10^6
k_4: q2 → c2	5.66×10^9
k_{-4}: c2 → q2	2.97×10^6
k_5: c5-cis → c5-trans	1.16×10^{13}
k_{-5}: c5-trans → c5-cis	2.81×10^{13}
k_6: c2 → c5-trans	9.46×10^6
k_{-6}: c5-trans → c2	8.58×10^7
k_7: c2 → c1	4.57×10^9
k_{-7}: c1 → c2	4.39×10^7
k_7: c6 → p1	3.21×10^8
k_8: c3 → p1	1.87×10^8
k_9: c5-cis → p1	2.04×10^9
k_{10}: c2 → p1	6.00×10^9
k_{11}: c2 → p3	8.90×10^6
k_{12}: c5-trans → p2	4.30×10^9
k_{13}: c1 → p3	5.14×10^6

[a] Computed at zero collision energy.

TABLE 3: Calculated Product Branching Ratios (%) in the C_2H + C_2H_4 Reaction[a]

product	branching ratio
vinylacetylene, p1 + H from c6	77.94
vinylacetylene, p1 + H from c3	21.06
vinylacetylene, p1 + H from c5-cis	0.12
vinylacetylene, p1 + H from c2	0.72
vinyl radical + acetylene, p2	0.10
butatriene, p3 + H	5.46×10^{-2}

[a] Computed at zero collision energy.

3.2. The C_2H_3 + C_2H_2 Reaction. While considering the C_2H_3 + C_2H_2 reaction, we adopted the same C_4H_5 isomer and product classification that was used to study C_2H + C_2H_4. Selected ZPE-corrected relative energies of C_4H_5 isomers and transition states with respect to C_2H_3 + C_2H_2 calculated at the CCSD(T)/cc-pVQZ//B3LYP/6-311G(d,p) level are presented in Table 4 along with B3LYP/6-311G(d,p) energies as well as the available data from ab initio calculations by Miller et al.[21] As in case of the C_2H + C_2H_4 reaction, we will rely here on CCSD(T) relative energies with ZPE corrections. Accordingly, the overall kinetic scheme of the C_2H_3 + C_2H_2 reaction extracted from the full graph of possible isomerization and dissociation pathways on the C_4H_5 PES is presented in Figure 6 and the most important dissociation channels are depicted in Figures 7 and 8. It appears that the reverse C_2H_3 + C_2H_2 reaction proceeds with entrance barriers of 6.0−6.1 kcal/mol depending on the initial adduct, thus being much less favorable than the barrierless

at about 1 mbar at 100 K and at higher pressures for warmer temperatures, whereas c6 can be stabilized at even higher pressures.

11124 *J. Phys. Chem. A, Vol. 113, No. 42, 2009*

Krishtal et al.

TABLE 4: Relative Energies (kcal/mol, with respect to C_2H_3 + C_2H_2) of Selected C_4H_5 and C_4H_4 Isomers and Transition States from B3LYP/6-311G(d,p) (ΔE_{B3LYP}) and CCSD(T)/ cc-pVQZ//B3LYP/6-311G(d,p) +ZPE ($\Delta E_{CCSD(T)}$) Calculations (presented here for comparison with the data from ref 21, $\Delta E_{CCSD(T)}$ for the other species can be obtained by adding the value of 22.2 to their relative energies in the C_2H + C_2H_4 reaction)

isomer/TS	ΔE_{B3LYP}	$\Delta E_{CCSD(T)}$	ΔE_{B3LYP} (ref 21)	ΔE_{G2} (ref 21)
c1	−57.7	−50.3	−52.1	−49.9
c2	−56.3	−47.8	−50.8	−47.6
c3	−54.1	−47.6	−48.4	−47.4
c4-cis	−43.1	−38.0	−37.1[a]	−36.3[a]
c4-trans	−42.5	−37.4		
c5-cis	−40.0	−35.4		
c5-trans	−39.5	−34.9		
c6-a	−36.9	−34.7		−33.9[a]
c6-b	−36.5	−33.9		
(C_2H + C_2H_4)-c4-trans	4.1	6.0	5.8[a]	5.9[a]
(C_2H + C_2H_4)-c5-trans	4.2	6.1		
c5-trans−q1	−5.1	−1.9	−6.1[a]	−5.7[a]
c5-cis−q1	−11.7	−8.2		
c4-cis−p1	1.9	1.2	2.5[a]	2.4[a]
5-cis−p1	2.4	1.6		
c5-trans−c2	4.5	7.5	7.0	7.6
c2−p1	−1.0	−2.4	−0.9	−2.5
c2−c1	−1.2	5.3	−0.4	5.1
c3−p1		1.8[b]	−1.2	−4.4
q1	−50.6	−46.4	−43.0	−45.8
p1 + H	−1.1	−4.3	−1.4[a]	−4.4[a]
p3 + H	2.4	3.3		

[a] In ref 21, relative energies for one of n-C_4H_5 and one of c6 isomers, one of C_4H_4 + H products as well as one of n-C_4H_5-q1 and one of n-C_4H_5-p1 transition states are presented. ΔE_{B3LYP} and ΔE_{G2} energies from ref 21 denote the results from B3LYP/ aug-cc-pvtz calculations and G2-type estimates to the QCISD(T)/ 6311++G(3df,2pd), respectively. [b] Taken from CCSD(T)/cc-pVQZ// MP2/6-311G(d,p) + ZPE computations.

C_2H + C_2H_4 reaction. Therefore, the kinetic scheme needed for calculations of rate constants and product branching ratios for C_2H_3 + C_2H_2 reaction will include relatively higher energy isomerization and dissociation pathways as compared to C_2H + C_2H_4. Meanwhile, very high energy isomers and pathways with very high barriers that are unlikely to be accessed under Titan's low temperature conditions were excluded as insignificant for the kinetics studies. In particular, while constructing the kinetic scheme for RRKM calculations, we neglected all C_4H_5 isomers, products, and pathways with relative energies above 11.1 kcal/mol—the relative energy of the transition state for the 1,2-H shift in c5-cis to form c6, which may be a significant isomerization step on the course of the C_2H_3 + C_2H_2 reaction.

Our studies revealed that the addition of C_2H_3 to C_2H_2 results in the formation of chain initial adducts c4-trans and c5-trans that are cis−trans conformations of n-C_4H_5. According to the potential energy diagram for the C_2H_3 + C_2H_2 reaction given by Miller et al.,[21] the initial adduct for this reaction was considered to be n-C_4H_5 E-1,3-butadien-1-yl designated as c4-cis in the present work. Assuming that Miller et al. made no distinction between different n-C_4H_5 conformers in their study (indeed, as seen in Figure 6, different n-C_4H_5 structures are very close in energy and easily isomerize to each other through cis−trans rearrangements with barrier heights of only ∼3−5 cal/mol—see the c4-trans−c4-cis, c5-trans−c5-cis, c4-trans−c5-trans, c4-cis−c5-cis channels), a comparison of relative energies for the initial adducts and the appropriate barrier heights can

be made. The agreement is satisfactory, taking into account the difference in the applied computational methods; the barrier heights for the initial adducts formation are 6.0 and 6.1 kcal/ mol in our study vs 5.78 (DFT B3LYP) or 5.92 (G2) kcal/mol from the work of Miller et al.;[21] the relative energies of four n-C_4H_5 isomers c4-cis, c4-trans, c5-cis, and c5-trans are −38.0, −37.4, −35.4, and −34.9, respectively, vs −37.8 (DFT B3LYP) or −36.31 (G2) kcal/mol for a single n-C_4H_5 isomer presented by Miller et al.[21] While there is an overall agreement between the calculated relative energies of isomers and transition states presented here and reported by Miller et al.[21] (see Table 4 for comparison), our study presents an extended picture of the C_4H_5 PES and includes additional reaction channels that are needed for a more complete general description of the C_2H_3 + C_2H_2 reaction.

According to Table 4 and the kinetic scheme shown in Figure 6, only vinylacetylene + H and butatriene + H may be considered as possible products of the C_2H_3 + C_2H_2 reaction. Methylenecyclopropene + H and C_2H + C_2H_4 lie 19.3 and 22.2 kcal/mol respectively higher in energy than the reactants and are unlikely to be formed through exit barrierless dissociation of c6, t2, or q2, which can in principle be produced from c4-trans and c5-trans via a set of intermediate isomerization steps. Miller et al.[21] considered only one C_4H_4 isomer (vinylacetylene) as a possible product, but we additionally included the pathways leading to butatriene. On the other hand, here we do not regard various C_4H_5 isomers as potential products because our goal is to model the C_2H_3 + C_2H_2 reaction under single-collision conditions of crossed molecular beams experiments or low-pressure environments in Titan's atmosphere, where the chemically activated C_4H_5 species are unlikely to be collisionally stabilized and therefore are destined to dissociate. Alternatively, Miller et al.'s consideration is pertinent to high temperatures and pressures that are typical for combustion processes where some of C_4H_5 radicals can be distinct reaction products.[21]

Formation of Vinylacetylene. In the C_2H_3 + C_2H_2 reaction, there are the same five dissociation channels resulting in the production of vinylacetylene occurring by the H loss from vicinal CH, CH$_2$, and terminal CH$_2$ and CH$_3$ groups in chain C_4H_5 isomers: c4-cis−p1, c5-cis−p1, c2−p1, c6−p1, and c3−p1. While a direct H elimination from c6 along with 1,2-H migration in the same isomer followed by H loss from the CH$_3$ group in c3 dominated the formation of vinylacetylene in the C_2H + C_2H_4 reaction considered above, the shortest pathways to p1 from C_2H_3 + C_2H_2 include two similar two-step channels starting with isomerizations of the initial adducts c4-trans and c5-trans to the corresponding cis conformations (c4-trans−c4-cis and c5-trans−c5-cis) followed by dissociation of the cis-conformers to C_4H_4 + H (c4-trans−c4-cis−p1 and c5-trans−c5-cis−p1). Note that these two channels are also very similar from the point of view of feasibility as they proceed via minima and saddle points having very close energy (within 3−5 kcal/mol), with the c4-trans−c4-cis−p1 channel being slightly more energetically preferable. The third two-step channel utilizes the structural features of c5-trans, namely, cis-arrangement of the terminal C atoms accompanied with H atoms in the acetylene-like fragment located in trans-orientation relative to the acetylenic CC bond. Such conformation allows the 1,2-H shift to proceed via a typical barrier of 42.4 kcal/mol resulting in c2, which further dissociates to C_4H_4 + H with an exit barrier of 1.9 kcal/mol—the corresponding transition state resides 2.4 kcal/ mol lower in energy than the reactants (c5-trans−c2−p1).

Being topologically close species with similar energies, the n-C_4H_5 conformers, c4-trans, c4-cis and c5-trans, c5-cis can also
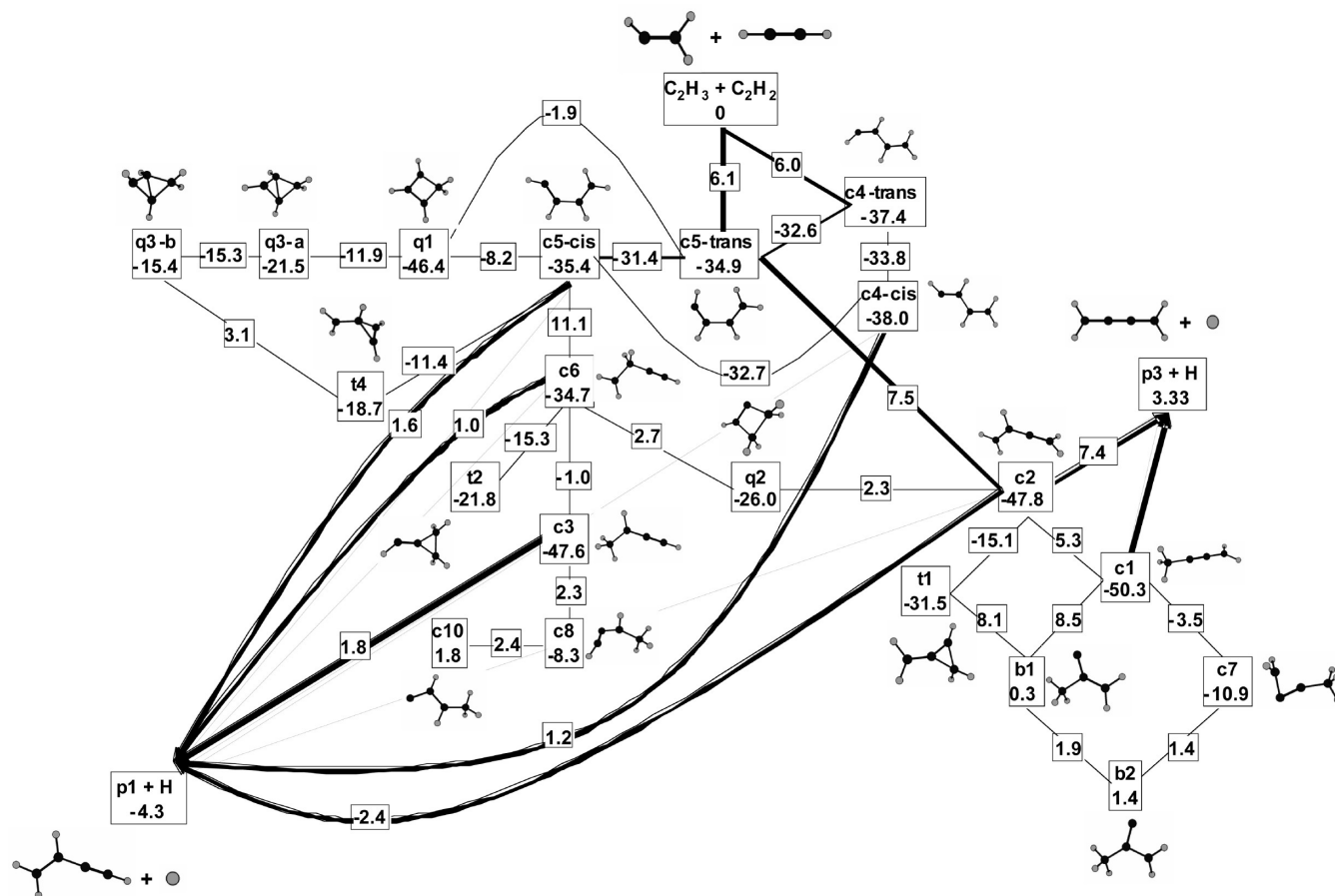
Figure 6. Overall kinetic scheme of the C$_2$H$_3$ + C$_2$H$_2$ reaction used in calculations of product branching ratios. Relative energies are taken from CCSD(T)/cc-pVQZ//B3LYP/6-311G(d,p) +ZPE calculations.

easily rearrange to each other, giving four competitive three-step channels connecting the initial adducts with the C$_4$H$_4$ + H products: c4-trans–c5-trans–c5-cis–p1, c5-trans–c4-trans–c4-cis–p1, c4-trans–c4-cis–c5-cis–p1, and c5-trans–c5-cis–c4-cis–p1. Alternative three-step channels to form vinylacetylene include the c4-trans–c5-trans conformational change by isomerization of c5-trans to c2 and H loss (c4-trans–c5-trans–c2–p1) and isomerization of the initial adduct c5-trans to its cis-conformer followed by 1,2-H shift to form c6 with the final H loss from the vicinal CH$_2$ group of c6 (c5-trans–c5-cis–c6–p1). Notably, this pathway includes the c6–p1 dissociation channel, which was found to be of key importance for the production of vinylacetylene in the C$_2$H + C$_2$H$_4$ reaction. Finally, for completeness we list possible four-step routes to C$_4$H$_4$ + H: c5-trans–c5-cis–c6–c3–p1, c4-trans–c5-trans–c5-cis–c6–p1, c4-trans–c4-cis–c5-cis–c6–p1, and c5-trans–c2–q2–c6–p1. There also exist several channels including five and more steps that are either combinations of the reaction channels considered above or proceed through cyclization of the initial c5-trans adduct or its cis-conformer to the four-member ring q1 isomer with further transformation of q1 back to c5-cis through the formation of bicyclic structures q3-a and q3-b and consecutive opening of two three-member rings with t4 being the intermediate between q3-b and c5-cis.

Formation of Butatriene. In contrast to the vinylacetylene + H products that are 4.3 kcal/mol lower in energy than C$_2$H$_3$ + C$_2$H$_2$, butatriene + H reside 3.3 kcal/mol above the reactants. Two possible pathways connecting the initial adducts with butatriene, namely, the c2–p3 channel with H loss from the vicinal CH group in c2 and c1–p3 with exit-barrier-less H elimination from the CH$_3$ group of c1 can be accessed only

through high-energy barriers for 1,2-H migration on the c5-trans–c2 and c5-cis–c6 stages, contrary to the formation of vinylacetylene proceeding via low-barrier conformational changes in the n-C$_4$H$_5$ isomers. Thus, because butatriene is expected to be a minor (or trace) product, we will briefly consider only those channels for its formation that are most important from the theoretical point of view. The two-step mechanism starts with the initial adduct c5-trans that undergoes 1,2-H migration to form c2 followed by H loss from CH (c5-trans–c2–p3). Alternative two three-step and one four-step routes are the following: c5-trans–c2 followed by another 1,2-H shift to form c1, which dissociates via exit-barrier-less exit channel c1–p3 (c5-trans–c2–c1–p3), c4-trans–c5-trans–c2–p3, and c4-trans–c5-trans–c2–c1–p3, which is a combination of the above. There also exist five and more step pathways connecting the initial adducts with the dissociation channels c2–p3 and c1–p3, which involve cis–trans isomerizations in n-C$_4$H$_5$ followed by c5-trans–c2 and c5-cis–c6–q2–c2 rearrangements. Finally, even longer routes include transformation of c2 to c1 through the formation of the branching structure b1 (with t1 serving as an intermediate), which can either directly isomerize to c1 by 1,2-CH$_3$ migration or produce, via an intermediate b2, an "improper" cyclic isomer c7 with nearly closed three-member ring then converting into c1.

Rate Constants and Product Branching Ratios. Energy-dependent RRKM rate constants were computed at two collision energies, 6.1 kcal/mol, which opens both reaction entrance channels, and 11.1 kcal/mol, to allow the c5-trans–c2, c5-cis–c6, and c2–p3 steps to occur. The calculated individual-step rate constants are shown in Table 5, and branching ratios are presented in Table 6 only for E_{col} = 11.1 kcal/mol because
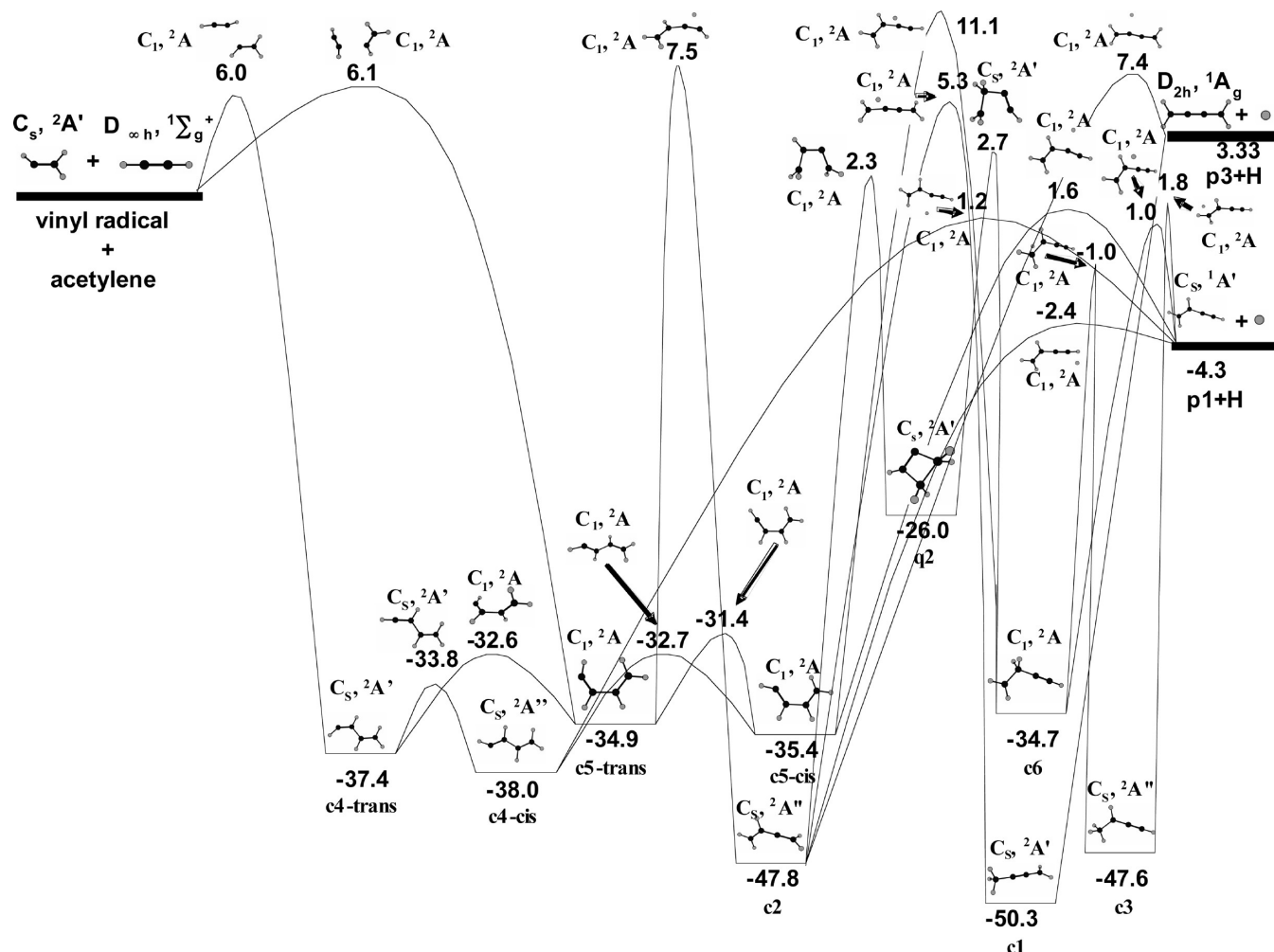
Figure 7. Potential energy diagram for the most important channels of the $C_2H_3+C_2H_2$ reaction.

the results for the two collision energies are nearly identical. One can see that that vinylacetylene is again practically the sole reaction product and it is produced either from c5-cis (~58%) or c4-cis (42%). The relative yields appear to be independent of the initial adduct, c4-trans or c5-trans. This can be explained by very fast isomerization between the n-C_4H_5 conformations. The isomerization barriers are very low, and the computed rate constants are in the range of 10^{12}–10^{13} s^{-1}, i.e., close to the applicability limit of RRKM theory. Therefore, the isomerization steps are several orders of magnitude faster than the H elimination from c5-cis or c4-cis and a steady-state equilibrium between the c4 and c5 conformers is achieved before they can lose a hydrogen atom. Interestingly, although the barrier for H loss from c5-cis is slightly (0.4 kcal/mol) higher than that from c4-cis, a higher yield of vinylacetylene is computed from c5-cis rather than from c4-cis. This can be understood if we look at the equilibrium between the two conformers. As seen in Table 5, rate constants k_5(c4-cis → c5-cis) and k_{-5}(c5-cis → c4-cis) are 1.69×10^{12} and 1.08×10^{12} s^{-1}, giving the equilibrium constant K(c4-cis → c5-cis) = 1.56. This means that when the equilibrium is established, the concentration of c5-cis is a factor of 1.56 that of c4-cis. After multiplying the rate constant k_8(c5-cis → p1), 6.48×10^7 s^{-1}, by this concentration factor, we obtain 1.01×10^8 s^{-1}, i.e., a faster rate constant than k_7(c4-cis → p1), 7.35×10^7 s^{-1}, and this simple consideration gives the branching ratio of the two channels as 58/42, close to the result obtained by the rigorous calculations (Table 6). So, the preference of the channel via c5-cis is explained by the fact that the c4-cis–c5-

cis equilibrium is shifted toward the latter. But why k_{-5} is slower than k_5 although the barrier for c4-cis → c5-cis is 2.6 kcal/mol higher than that for the reverse reaction and c4-cis is more energetically more stable than c5-cis? The explanation comes from the analysis of the density of states for the two isomers. c5-cis is looser and has the lowest vibrational frequency of 65 cm^{-1}, almost three times smaller than that for c4-cis, 178 cm^{-1}, with all other frequencies being similar. Therefore, at the available internal energy, the density of states of c5-cis is higher than that of c4-cis, just overcompensating for the energetic preference of the latter.

4. Conclusions

Detailed and extensive ab initio calculations of various stationary points on the C_4H_5 global PES allowed us to theoretically unravel the $C_2H + C_2H_4$ and $C_2H_3 + C_2H_2$ reaction mechanisms under single-collision conditions. The results predict vinylacetylene + H to be the nearly exclusive products for both reactions. The exothermicities of these products with respect to ethynyl + ethylene and vinyl + acetylene are computed to be 26.5 and 4.3 kcal/mol, respectively. The most important mechanisms for $C_2H + C_2H_4$ include a barrierless formation of the chain CH_2CH_2CCH adduct c6 in the entrance channel (56.9 kcal/mol below the reactants) followed either by direct H loss from the vicinal CH_2 group via a barrier of 35.7 kcal/mol (exit barrier of 5.3 kcal/mol) or by 1,2-H migration to form CH_3CHCCH c3 (69.8 kcal/mol lower in energy than C_2H

Product Branching Ratios of $C_2H + C_2H_4$

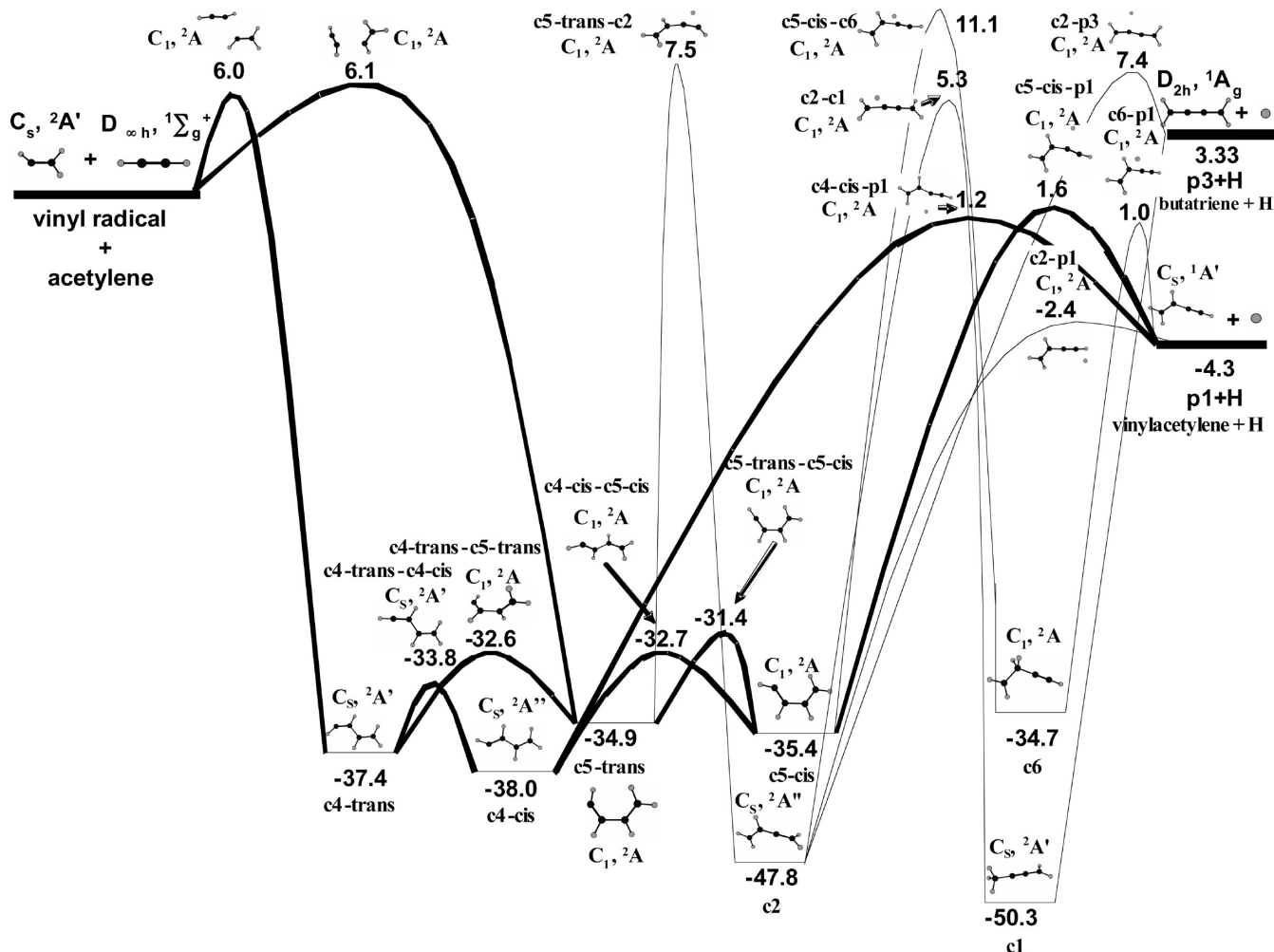*J. Phys. Chem. A, Vol. 113, No. 42, 2009* **11127**

Figure 8. $C_2H_3 + C_2H_2$ reaction channels used in calculations of rate constants and product branching ratios. The most important reaction routes are shown by bold lines.

TABLE 5: Microcanonical Rate Constants (s^{-1}) for Unimolecular Reaction Channels Used for Calculations of Product Branching Ratios for the $C_2H_3 + C_2H_2$ Reaction

channel	rate constant (collision energy 6.1 kcal/mol)	rate constant (collision energy 11.1 kcal/mol)
k_1: c4-trans → c5-trans	1.50×10^{12}	1.65×10^{12}
k_{-1}: c5-trans → c4-trans	2.27×10^{12}	2.39×10^{12}
k_2: c4-trans → c4-cis	7.06×10^{13}	7.73×10^{12}
k_{-2}: c4-cis → c4-trans	6.45×10^{12}	7.12×10^{12}
k_3: c5-trans → c5-cis	2.15×10^{13}	2.37×10^{13}
k_{-3}: c5-cis → c5-trans	8.72×10^{12}	9.68×10^{12}
k_4: c5-trans → c2	0	4.25×10^{5}
k_{-4}: c2 → c5-trans	0	3.29×10^{4}
k_5: c4-cis → c5-cis	1.51×10^{12}	1.69×10^{12}
k_{-5}: c5-cis → c4-cis	1.02×10^{12}	1.08×10^{12}
k_6: c5-cis → c6	0	1.16×10^{3}
k_{-6}: c6 → c5-cis	0	5.13×10^{2}
k_7: c2 → c1	2.25×10^{3}	3.48×10^{5}
k_{-7}: c1 → c2	6.00×10^{1}	9.54×10^{3}
k_7: c4-cis → p1	4.82×10^{6}	7.35×10^{7}
k_8: c5-cis → p1	3.89×10^{6}	6.48×10^{7}
k_9: c2 → p1	3.13×10^{7}	2.75×10^{8}
k_{10}: c2 → p3	0	2.39×10^{4}
k_{11}: c6 → p1	9.35×10^{5}	1.22×10^{7}
k_{12}: c1 → p3	7.03×10^{3}	1.65×10^{5}

TABLE 6: Calculated Product Branching Ratios (%) in the $C_2H_3 + C_2H_2$ Reaction^a

| product	branching ratio
vinylacetylene, p1 + H from c4-cis	42.00
vinylacetylene, p1 + H from c5-cis	57.84
vinylacetylene, p1 + H from c2	0.15
vinylacetylene, p1 + H from c6	1.03×10^{-3}
butatriene, p3 + H	1.98×10^{-4}

^{a} Computed at collision energy of 11.1 kcal/mol.

dependent rate constants for individual reaction step and branching ratios for various channels indicate that 77−78% of vinylacetylene is formed directly from the initial adduct, whereas 22−21% are produced via the two-step mechanism involving the 1,2-H shift c6−c3, with alternative channels contributing less than 1%. The other products, $C_2H_3 + C_2H_2$, butatriene + H, or methylelenecyclopropene + H, can be formed only in negligibly small amounts if the $C_2H + C_2H_4$ reaction follows statistical behavior. The theoretical results support the experimental crossed molecular beams observations of vinylacetylene being the major product of the $C_2H + C_2H_4$ reaction and the fact that CH$_2$CHCCH is formed via a tight exit transition state and confirm that vinylacetylene can be produced from $C_2H + C_2H_4$ under low temperature conditions of Titan's atmosphere.

The prevailing mechanism for the $C_2H_3 + C_2H_2$ reaction begins with the initial formation of different n-C_4H_5 conformations occurring with significant entrance barriers of ~6 kcal/

+ C_2H_4) via a 33.8 kcal/mol barrier and H elimination from the terminal CH$_3$ group occurring with a barrier of 49.4 kcal/mol (exit barrier of 6.1 kcal/mol). RRKM calculations of energy-
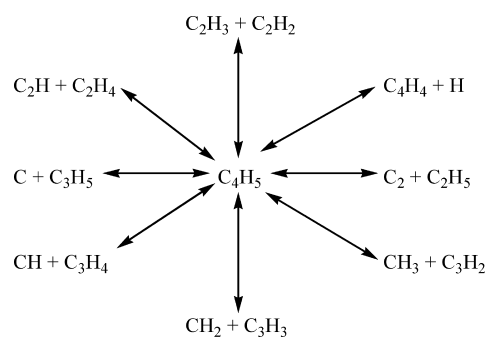
11128 *J. Phys. Chem. A, Vol. 113, No. 42, 2009*

Krishtal et al.

SCHEME 1

mol. The *n*-C$_4$H$_5$ isomers reside 35−38 kcal/mol lower in energy than C$_2$H$_3$ + C$_2$H$_2$ and can rapidly rearrange to one another overcoming relatively low barriers of 3−5 kcal/mol. H loss from the c4-cis and c5-cis C$_4$H$_5$ conformers then gives the vinylacetylene product via exit barriers of 5.5 and 5.9 kcal/mol with the corresponding transition states lying 1.2 and 1.6 kcal/mol above the C$_2$H$_3$ + C$_2$H$_2$ reactants, respectively. Since the reaction is hindered by relatively high entrance barriers, it is not expected to be important in Titan's atmospheric environments but can produce *n*-C$_4$H$_5$ or vinylacetylene under high temperature and pressure combustion conditions. The reaction can generate vinylacetylene + H under single-collision conditions only if the collision energy exceeds the entrance barrier height of ∼6 kcal/mol.

Some other chemical reactions can also access the C$_4$H$_5$ PES. For instance, the reaction of a carbon atom in its ground ^{3}P state with allyl radical C$_3$H$_5$ was studied earlier by ab initio/ RRKM calculations in our group.[16] The main difference between C (^{3}P) + C$_3$H$_5$ and the reactions considered in the present study is that the former can produce both vinylacetylene + H and C$_2$H$_3$ + C$_2$H$_2$ in comparable yields depending on the branching in the entrance channel,[16] whereas C$_2$H + C$_2$H$_4$ and C$_2$H$_3$ + C$_2$H$_2$ form only the former product. In addition, the barrierless C (^{3}P) + C$_3$H$_5$ → C$_4$H$_4$ + H/C$_2$H$_3$ + C$_2$H$_2$ reaction exhibits much higher exothermicities in the range of 86−91 kcal/mol. The calculated C$_4$H$_5$ surface also helps to realize that the isomerization of butatriene and methylenecyclopropene C$_4$H$_4$ isomers to the most stable vinylacetylene structure can be catalyzed by an H radical. In particular, the highest barriers on the rearrangement pathways from p3 and p4 to p1 were earlier calculated to be ∼73 and 42 kcal/mol.[34] However, if a free hydrogen atom is available, the H-catalyzed butatriene−vinylacetylene isomerization can proceed as p3 + H → c1 → c2 → p1 + H with the highest energy transition state for the c1−c2 step residing only 1.9 kcal/mol above the reactants or as p3 + H → c2 → p1 + H with the highest barrier of 4.1 kcal/mol. Similarly, the H-assisted methylenecyclopropene−vinylacetylene reaction can take the following barrier-free pathway, p4 + H → t1 → c2 → p1 + H, with all intermediates and transition states lying below the reactants. Therefore, in the presence of H atoms, butatriene can only be stable at low temperatures, whereas methylenecyclopropene would rapidly interconvert to vinylacetylene.

In summary, as illustrated in Scheme 1, the global C$_4$H$_5$ PES is relevant to many important reactions.

In addition to the C$_2$H + C$_2$H$_4$, C$_2$H$_2$ + C$_2$H$_3$, C$_4$H$_4$ + H, and C + C$_3$H$_5$ considered here and earlier, several other reactions, including CH + C$_3$H$_4$ (allene and methylacetylene),

CH$_2$ + C$_3$H$_3$, CH$_3$ + C$_3$H$_2$, and C$_2$ + C$_2$H$_5$ can be analyzed in the future after examining their entrance channels into the C$_4$H$_5$ surface.

References and Notes

(1) Wilson, E. H.; Atreya, S. K.; Coustenis, A. *J. Geophys. Res.* **2003**, *108*, 5014–5023.

(2) Miller, J. A.; Melius, C. F. *Combust. Flame* **1992**, *91*, 21–39.

(3) Callear, A. B.; Smith, G. B. *Chem. Phys. Lett.* **1984**, *105*, 119–122.

(4) Chastaing, D.; James, P. L.; Sims, I. R.; Smith, I. W. M. *Faraday Discuss.* **1998**, *109*, 165–181.

(5) Mebel, A. M.; Kislov, V. V.; Kaiser, R. I. *J. Am. Chem. Soc.* **2008**, *130*, 13618–13629.

(6) Walch, S. P. *J. Chem. Phys.* **1995**, *103*, 8544–8547.

(7) Kaiser, R. I.; Stranges, D.; Bevsek, H. M.; Lee, Y. T.; Suits, A. G. *J. Chem. Phys.* **1997**, *106*, 4945–4953.

(8) Madden, L. K.; Moskaleva, L. V.; Kristyan, S.; Lin, M. C. *J. Phys. Chem. A* **1997**, *101*, 6790–6797.

(9) Cavallotti, C.; Rota, R.; Carra, S. *J. Phys. Chem. A* **2002**, *106*, 7769–7778.

(10) Kunde, V. G.; Aikin, A. C.; Hanel, R. A.; Jennings, D. E.; Maguire, W. C.; Samuelson, R. E. *Nature* **1981**, *292*, 686–688.

(11) Waite, J. H.; Cravens, T. E.; Ip, W.; Kaspizak, W.; Luhmann, J.; McNutt, R.; Niemann, H.; Yelle, R.; Wordag-Muller, I.; Ledvina, S.; Haye, V. D. *Cassini-Huygens Ion Neutral Mass Spectrometer: Early Saturn and Titan Results. Proceedings of the 36th DPS Meeting.* **2004**, *36*, 1068.

(12) (a) Landera, A.; Krishtal, S. P.; Kislov, V. V.; Mebel, A. M.; Kaiser, R. I. *J. Chem. Phys.* **2008**, *128*, 214301. (b) Landera, A.; Mebel, A. M.; Kaiser, R. I. *Chem. Phys. Lett.* **2008**, *459*, 54–59.

(13) Zhang, F. Kim, S. Kaiser, R. I. Krishtal, S. P. Mebel, A. M. *J. Phys. Chem. A*, DOI: 10.1021/jp9032595, in this issue.

(14) Parker, C. I.; Cooksy, A. I. *J. Phys. Chem. A* **1998**, *102*, 6186–6190.

(15) Parker, C. I.; Cooksy, A. I. *J. Phys. Chem. A* **1999**, *103*, 2160–2169.

(16) Nguyen, T. L.; Mebel, A. M.; Kaiser, R. I. *J. Phys. Chem. A* **2003**, *107*, 2990–2999.

(17) Wheeler, S. E.; Allen, W. D.; Schaefer, H. F., III. *J. Chem. Phys.* **2004**, *121*, 8800–8813.

(18) Hansen, N.; Klippenstein, S. J.; Taatjes, C. A.; Miller, J. A.; Wang, J.; Cool, T. A.; Yang, B.; Yang, R.; Wei, L.; Huang, C.; Wang, J.; Qi, F.; Law, M. E.; Westmoreland, P. R. *J. Phys. Chem. A* **2006**, *110*, 3670–3678.

(19) Woon, D. E. Park, J.-Y. *Icarus* DOI: 10.1016/j.icarus.2009.02.028.

(20) Wang, H.; Frenklach, M. *J. Phys. Chem.* **1994**, *98*, 11465–11489.

(21) Miller, J. A.; Klippenstein, S. J.; Robertson, S. H. *J. Phys. Chem. A* **2000**, *104*, 7525–7536.

(22) Becke, A. D. *J. Chem. Phys.* **1993**, *98*, 5648–5652.

(23) Lee, C.; Yang, W.; Parr, R. G. *Phys. Rev. B* **1988**, *37*, 785–789.

(24) Krishnan, R.; Frisch, M.; Pople, J. A. *J. Chem. Phys.* **1980**, *72*, 4244–4245.

(25) Purvis, G. D.; Bartlett, R. J. *J. Chem. Phys.* **1982**, *76*, 1910–1918.

(26) (a) Dunning, T. H., Jr. *J. Chem. Phys.* **1989**, *90*, 1007–1023. (b) Woon, D. E.; Dunning, T. H., Jr. *J. Chem. Phys.* **1993**, *98*, 1358–1371.

(27) Frisch, M. J.; Trucks, G. W.; Schlegel, H. B.; et al. *GAUSSIAN 98, Revision A.9*; Gaussian Inc.; Pittsburgh, PA, 1998.

(28) Werner, H.-J.; Knowles, P. J.; Lindh, R.; et al. *MOLPRO, Version 2002.6*, University of Birmingham: Birmingham, U.K., 2003.

(29) Eyring, H.; Lin, S. H.; Lin, S. M. *Basic Chemical Kinetics*; Wiley: New York, 1980.

(30) Stein, S. E.; Rabinovitch, B. S. *J. Phys. Chem.* **1973**, *58*, 2438.

(31) Steinfield, J. I.; Francisco, J. S.; Hase, W. L. *Chemical Kinetics and Dynamics*; Prentice Hall: Engelwood Cliffs, NJ, 1999.

(32) Kühnel, W.; Gey, E.; Ondruschka, B. Z. *Z. Phys. Chem. (Leipzig)* **1987**, *268*, 23–32.

(33) Kühnel, W.; Gey, E.; Ondruschka, B. Z. *Z. Phys. Chem. (Leipzig)* **1987**, *268*, 805–814.

(34) Mebel, A. M.; Kislov, V. V.; Kaiser, R. I. *J. Chem. Phys.* **2006**, *125*, 133113.

JP904033A